

1 **Root water uptake patterns are controlled by tree species**

2 **interactions and soil water variability**

3 Gökben Demir¹, Andrew J. Guswa², Janett Filipzik¹, Johanna Clara Metzger^{1,3}, Christine Römermann^{4,6},
4 Anke Hildebrandt^{1,5,6}

5 ¹ Group of Terrestrial Ecohydrology, Institute of Geoscience, Friedrich Schiller University Jena, Jena,
6 07749, Germany

7 ² Picker Engineering Program, Smith College, Northampton, MA, 01063, USA

8 ³Institute of Soil Science, University of Hamburg, Hamburg, 20146, Germany

9 ⁴Plant Biodiversity, Institute of Ecology and Evolution, Friedrich Schiller University Jena, Jena, 07743,
10 Germany

11 ⁵ Department of Computational Hydrosystems, Helmholtz Centre for Environmental Research – UFZ,
12 Leipzig, 04318, Germany

13 ⁶German Centre for Integrative Biodiversity Research (iDiv) Halle -Jena-Leipzig, Leipzig, 04103,
14 Germany

15
16 Correspondence to: goekben.demir@uni-jena.de and anke.hildebrandt@ufz.de

17 **Abstract**

18 Throughfall is the largest source of water entering the soil in forests, and its spatial distribution depends
19 on several biotic and abiotic factors. It is well documented that the distribution of throughfall results in
20 reoccurring higher and lower water inputs at certain locations. However, the role of horizontal root water
21 uptake patterns in understanding the effects of throughfall patterns on subsurface water dynamics remains
22 unresolved. Therefore, we investigate root water uptake patterns by considering spatial patterns of
23 throughfall and soil water patterns in addition to soil and neighboring tree characteristics. In a beech-
24 dominated mixed deciduous forest in a temperate climate, we conducted weekly intensive throughfall
25 sampling at locations paired with soil moisture sensors during the 2019 growing season. We employed a
26 linear mixed-effects model to understand controlling factors for root water uptake patterns. Our results
27 show that soil water patterns and interactions among neighbouring trees are the most significant factors
28 regulating root water uptake patterns. Temporally stable throughfall patterns did not influence root water
29 uptake patterns. Similarly, soil properties were unimportant for spatial patterns of root water uptake. We

30 found that wetter locations (rarely associated with throughfall hotspots) promoted greater root water
31 uptake. Root water uptake in monitored soil layers also increased with neighbourhood species richness.
32 Ultimately our findings suggest that complementarity mechanisms within the forest stand, in addition to
33 soil water variability and availability, govern root water uptake patterns.

34

35 **Key words:** root water uptake, throughfall, soil water, spatial patterns, beech

36 **1) Introduction**

37 Vegetation intercepts and redirects precipitation into throughfall and stemflow, collectively referred to as
38 below-canopy precipitation. Throughfall is typically the largest component of below canopy precipitation
39 (Levia and Frost, 2006; Sadeghi et al., 2020). For instance, in temperate forests about 70% of above
40 canopy precipitation ends up as throughfall (Levia and Frost, 2003; Sadeghi et al., 2020). Hence,
41 throughfall serves as the primary source for replenishing soil moisture in vegetated areas.

42 Below-canopy precipitation is modified by several biotic and abiotic factors (Levia and Frost, 2006; Levia
43 et al., 2011), including vegetation type, canopy architecture (Crockford and Richardson, 2000; Pypker et
44 al., 2011; Levia et al., 2017), and forest structure (Rodrigues et al., 2022), meteorological elements such
45 as wind speed (Staelens et al., 2008; Van Stan et al., 2011; Fan et al., 2015), precipitation intensity and
46 event size (Dunkerley, 2014; Magliano et al., 2019; Zhang et al., 2016; Staelens et al., 2008). As a result,
47 throughfall inherently varies across space and time. However, previous studies showed that the spatial
48 distribution of throughfall persists over time (Keim et al., 2005; Staelens et al., 2006; Guswa and Spence,
49 2012; Carlyle-Moses et al., 2014; Metzger et al., 2017; Van Stan et al., 2020).

50 Throughfall patterns potentially translate the spatial variability of water inputs into soil moisture (Raat et
51 al., 2002; Blume et al., 2009; Zimmermann et al., 2009; Zehe et al., 2010; Bachmair et al., 2012;
52 Rosenbaum et al., 2012; Zhang et al., 2016). A decade ago Coenders-Gerrits et al., (2013) proposed that
53 throughfall patterns are translated into soil wetting dynamics with a model based on combined hillslope
54 topographic and throughfall data collected in a beech-dominated catchment. However, in this model, the
55 effect of throughfall patterns on soil moisture patterns rapidly ceased. Later, Metzger et al. (2017)

56 empirically confirmed that throughfall patterns barely alter soil moisture response to rainfall, and this
57 limited influence rapidly disappears. More recently, Zhu et al. (2021) observed that stable spatial patterns
58 of throughfall were weakly related to the spatial distribution of soil moisture since this relationship was
59 restricted only to relatively wet soil locations and throughfall hotspots. They also showed that throughfall
60 patterns had a weak influence on the temporal dynamics of soil water content compared to soil bulk
61 density and litter layer properties.

62 Previous studies have suggested that soil properties (Metzger et al., 2017), preferential flow (Jost et al.,
63 2004; Blume et al., 2009; Molina et al., 2019; Fischer-Bedtke et al., 2023), and litter layer processes (Raat
64 et al., 2002) may result in weak and short-term effects of throughfall patterns on soil moisture variability.
65 Regardless, Fischer-Bedtke et al., (2023) found that recurring throughfall patterns left a notable imprint
66 on soil moisture, although the effect on absolute values of soil water content after drainage was rather
67 weak. There, other factors such as soil macroporosity, distance from the tree and other processes, namely
68 fast flow,, more strongly influenced soil moisture patterns. Based on a one-dimensional soil-water model,
69 Bouten et al. (1992) proposed that throughfall patterns alter and localize root water uptake as well as
70 promote fast drainage. However, to the best of our knowledge, the feedback mechanism of throughfall
71 patterns on root water uptake variation has not yet been investigated in the field. Therefore, it is unclear
72 how water uptake patterns play a role in translating throughfall patterns into spatio-temporal variation of
73 soil water and vice versa.

74 In addition to spatial variation of throughfall and soil moisture, soil properties are among the abiotic
75 factors that may alter root water uptake patterns (Nadezhdina et al., 2007; Kirchen et al., 2017). For given
76 evaporative demand, water uptake at a particular location is a function of water transport resistance
77 between root and soil in addition to the soil-water potential (Cardon and Letey, 1992; Shani and Dudley,
78 1996; Lhomme, 1998). Both characteristics depend on local soil properties and soil water status, and the
79 latter in turn is affected by the local water uptake rate. Soil moisture variability may shape root water
80 uptake patterns even more than root networks (Kühnhammer et al., 2020; Guderle et al., 2018). On the
81 flip side, root water uptake can amplify or homogenize soil moisture variability (Hupet and Vanclooster,
82 2005; Teuling and Troch, 2005; Ivanov et al., 2010; Baroni et al., 2013; Martínez García et al., 2014).
83 Soil properties control soil water redistribution (Grayson et al., 1997; Cosh et al., 2008; Jarecke et al.,

84 2021) and water availability for root structures (Vereecken et al., 2007; Cai et al., 2018). Moreover,
85 variations in soil water content reflect root water uptake (Hupet et al., 2002; Schume et al., 2004;
86 Schwärzel et al., 2009; Guderle and Hildebrandt, 2015; Jackisch et al., 2020).

87 Temporal and diurnal changes in local soil water content can be employed to quantify root water uptake
88 by dissecting soil water flow and water uptake under meteorological conditions that ensure transpiration
89 demand (Guderle and Hildebrandt, 2015; Jackisch et al., 2020; Hupet et al., 2002). Other methods,
90 especially using tracers, exist to evaluate the spatial distribution of root water uptake. Specifically, stable
91 water isotopes can be used to estimate water sources for water uptake by comparing the isotopic
92 composition of plant xylem water to that of potential water sources using different methods including
93 graphical inference, end-member mixing models, multi-source linear mixing models, and physically
94 based analytical models (Rothfuss and Javaux, 2017). In addition, tracking isotopically enriched water
95 can assist in the determination of water uptake dynamics (e.g., Zarebanadkouki et al., 2013). In contrast
96 to these methods, daily fluctuations in soil water allow for estimating the spatial distribution of ecosystem
97 evapotranspiration using standard measurements of soil water content (Guderle and Hildebrandt, 2016)
98 without the need for additional infrastructure.

99 Root networks can also regulate soil moisture distribution by transporting water from wetter places to
100 drier locations, which has been observed in a variety of ecosystems (e.g., Emerman and Dawson, 1996;
101 Katul and Siqueira, 2010; Yu and D'Odorico, 2015; Priyadarshini et al., 2016; Hafner et al., 2017). In
102 addition, tree size, age and species richness affect the spatio-temporal variation in root water uptake
103 (Volkman et al., 2016; Spanner et al., 2022; Kostner et al., 2002; Dawson, 1996; Brinkmann et al., 2019;
104 Gaines et al., 2016). Neighboring tree species with different hydraulic strategies may extract water from
105 different soil regions (Silvertown et al., 2015; Guo et al., 2018; Brum et al., 2019), and therefore more
106 diverse forest stands can be more resilient under drought stress (Pretzsch et al., 2013). However, soil
107 water scarcity during droughts can initiate or enhance competition mechanisms for water among different
108 tree species (González de Andrés et al., 2018; Vitali et al., 2018; Magh et al., 2020). Furthermore, studies
109 conducted in temperate forest ecosystems have demonstrated that the relationship between tree species
110 richness and water uptake varies (Krämer and Hölscher, 2010; Kunert et al., 2012; Meißner et al., 2012;
111 Forrester, 2014; Lübbe et al., 2016).

112 Taken together, throughfall and soil water variability, soil properties, and root water uptake patterns form
113 complex and intertwined interactions in the terrestrial hydrological cycle. It has not yet been shown
114 empirically how root water uptake patterns are affected by throughfall and spatial distribution of soil
115 water content. In line with previous modeling results (Bouten et al., 1992; Coenders-Gerrits et al., 2013)
116 we hypothesize that throughfall hotspots enhance water availability at certain locations that elevate root
117 water uptake. Further we investigate the role of soil water variation in combination with soil properties
118 and neighboring tree characteristics on root water uptake patterns. We pose the following questions to
119 test the main hypothesis and guide the investigation:

- 120 i) How do throughfall patterns influence root water uptake patterns?
- 121 ii) How does soil moisture and its variation, along with soil properties, control variation in root
122 water uptake?
- 123 iii) What is the role of biotic factors, namely size, distance, number, and species richness of
124 neighbouring trees on root water uptake patterns?

125 Here, we address these questions by employing a linear mixed effects model based on weekly throughfall
126 sampling at locations paired with intensive soil moisture measurements in a beech-dominated unmanaged
127 forest. We estimate root water uptake using a water balance method applied at soil moisture measurement
128 point. In addition, we incorporate data on field capacity, bulk density, and neighboring tree characteristics
129 namely size and species

130 **2) Materials and Methods**

131 **2.1) Research Site and Field Sampling**

132 **2.1.1) Research Site**

133 The research site is located in the forested upper hill region of the Hainich low mountain range in
134 Thuringia, Germany, as a part of the Hainich Critical Zone Exploratory (CZE) (Küsel et al., 2016). The
135 altitude in the research site ranges from 362 m to 368 m a.s.l. Mean annual air temperature varies between
136 7.5 and 9.5 °C, and the mean annual precipitation ranges from less than 600 to 1000 mm in the CZE
137 (Küsel et al., 2016).

138 In the study area, thin-bedded alternations of limestones and marlstones of carbonate rock (Middle
139 Triassic) form the bedrock overlain by a shallow Pleistocene loess layer with cambisols and luvisols as
140 dominant soil types (IUSS Working Group, 2006; Metzger et al., 2021). The median soil depth above the
141 weathered bedrock is 37 cm, with soil depths ranging from 15 cm to a maximum depth of 87 cm (Metzger
142 et al., 2017).

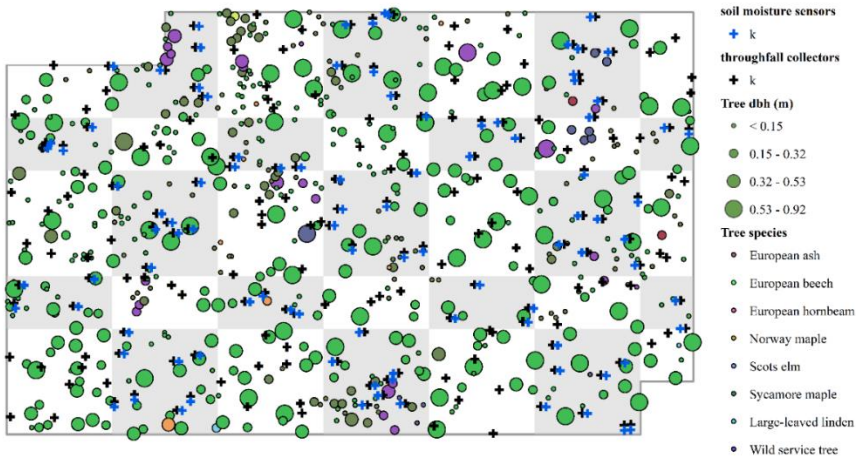
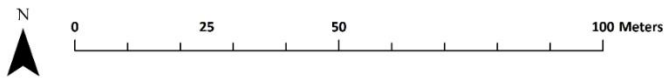
143 In 2019, the tree community in the research site consisted of 574 individuals of various ages (diameter at
144 breast height \geq 5cm). The dominant species is European beech (*Fagus sylvatica* L.), which makes up 70%
145 of the tree community, followed by sycamore maple (*Acer pseudoplatanus* L.) with 21 %, and European
146 ash (*Fraxinus excelsior* L.) with 4%. These dominant species are accompanied by Large-leaved linden
147 (*Tilia platyphyllos* Scop.), European hornbeam (*Carpinus betulus* L.), Norway maple (*Acer platanoides*
148 L.), Scots elm (*Ulmus glabra* L.), and Wild service tree (*Sorbus torminalis* (L.) Crantz). The stand has a
149 total basal area of 40 m² ha⁻¹ and has been unmanaged since 1997 (Kohlhepp et al., 2017).

150 **2.1.2) Soil moisture monitoring and soil properties**

151 The forest site (1 ha) was equipped with a soil moisture monitoring network (SoilNet; Bogena et al., 2010)
152 consisting of SMT100 frequency domain sensors (Treuebner GmbH, Neustadt, Germany). Metzger et al.
153 (2017) first described the soil moisture monitoring setup. Briefly, the observation platform (Figure 1) was
154 divided into 100 subplots (10 m \times 10 m), and 49 subplots were equipped with soil moisture sensors at
155 two random measuring points each, for a total of 98 locations. At each measuring point, sensors were
156 placed at two different depths, 7.5 cm (top sensors) and 27.5 cm (bottom sensors). The soil moisture
157 network is maintained through a regular bi-weekly routine to avoid potential failures such as depleted
158 sensors batteries, hardware problems, etc.

159 Undisturbed soil samples were collected during the sensor installation in 2014 and 2015 to estimate bulk
160 density and water content at field capacity. In addition, we collected additional disturbed soil samples (n
161 = 40) near sensor locations in 2019. Bulk density was determined from oven-dried (24h, 105°C) soil mass
162 weight and water content at field capacity by applying 60 hPa pressure to the saturated undisturbed sample
163 for 72 h.

164 Soil properties vary slightly from top to subsoil at the research site. While silty loam is the dominant soil
165 texture in both layers, the clay content is higher in the subsoil (Metzger et al., 2021). The median
166 volumetric water content at field capacity is 44% in the topsoil and 42% in the subsoil. Moreover, the
167 water content at field capacity varies from 27% to 60% and from 31% to 62% in the topsoil and subsoil,
168 respectively. The average bulk density (d_{bulk}) of the topsoil is 1.16 g cm^{-3} , with a range of 0.73 to 1.5 g
169 cm^{-3} . In the subsoil, the average bulk density (d_{bulk}) is slightly higher at 1.37 g cm^{-3} but has a similar range
170 ($0.7 - 1.6 \text{ g cm}^{-3}$) (See supplement for details).



171

172

173

174

175

Figure 1 (above) The photo of the site. (below) the field monitoring setup of stratified randomly distributed throughfall collectors and soil moisture sensors together with the trees which are sized according to the diameter at breast height (dbh) and coloured according to the species. Throughfall collectors are paired with soil moisture sensors at 98 locations (n=182) in the grey shaded subplots. White coloured subplots are equipped with only throughfall collectors.

176 **2.1.3) Gross precipitation and throughfall sampling**

177 Five gross precipitation funnels were placed 1.5 m above ground level in an adjacent open grassland (ca.
178 250 m distance to the research site). As described in Metzger et al. (2017) and Demir et al. (2022), the
179 precipitation funnels were made of a circular plastic funnel (12 cm in diameter) and sampling bottle (2 L
180 in volume), and ping pong balls were placed in the funnel orifice to prevent evaporation losses.

181 During the early growing season of 2019, we placed throughfall collectors in soil moisture monitoring
182 subplots at 98 locations. We paired these throughfall collectors with the soil moisture sensors by placing
183 them within 1 m of each other. The paired collectors were placed down-slope to avoid interference with
184 soil moisture measurements. For the rest of the research site, in 51 other subplots, we adopted a separate
185 independent stratified random design from Metzger et al. (2017). Briefly, we placed two throughfall
186 collectors in each subplot that was not equipped with soil moisture sensors. All throughfall collectors
187 were placed roughly 37 cm above the ground.

188 We conducted weekly manual measurement of throughfall and gross precipitation during the 2019
189 growing season (April to August). Sampling was conducted on rain free days only. Thus, the sampling
190 interval ranged between six and eight days..

191 We used the paired throughfall collectors (n = 98) to identify the drivers of root water uptake patterns, as
192 we derived root water uptake values based on soil water content measurements (see below). However, we
193 used all randomly placed throughfall collectors (n = 200) to describe the spatio-temporal variation of
194 throughfall within the research site.

195 **2.2) Estimation of potential evapotranspiration**

196 We calculated the daily potential evapotranspiration by applying the concept of thermodynamic limits of
197 convection (Kleidon and Renner, 2013; Kleidon et al., 2014):

$$198 \quad E_{\text{pot}} = \frac{1}{\lambda} \frac{s}{s+\gamma} \frac{R_{\text{sn}}}{2} \quad (1)$$

199 Where R_{sn} is absorbed solar radiation (W m^{-2}), λ is the latent heat of vaporization ($2.5 \times 10^6 \text{ Jkg}^{-1}$), γ is
200 the psychrometric constant (65 PaK^{-1}), and s is the slope of the saturation vapor pressure curve (PaK^{-1}).

201 Here, we acquired solar radiation, air temperature, and precipitation data for the throughfall sampling
202 period from a nearby weather station ("Reckenbuel") which is located approximately 1.4 km northeast of
203 the research site and provides data in 10 minutes intervals. The site-specific albedo for the summer period
204 was adopted from Otto et al. (2014).

205 We used the precipitation data measured at the weather station to define rain events and dry periods, as
206 described below.

207 **2.3) Data analysis**

208 **2.3.1) Quality control of soil water content data**

209 We systematically reviewed the six-minute soil water content data for quality control in two steps: 1)
210 identification of problems (such as jumps to extremely low and high values, duplicated time stamps of
211 different values, long discontinuities in the measurements, and lack of temporal variation in the time series
212 despite rain events), 2) classification and removal of detected outliers and irregularities. We visually
213 identified and removed unrealistic measurements such as extremely low (< 5 vol-%) and high values far
214 beyond the field capacity (> 75 vol-%) and long plateaus of repeated values despite rain events. We also
215 excluded any time series that exhibited long-term discontinuities that prevented us from calculating root
216 water uptake. During the visual inspection, we eliminated values with duplicated time stamps that violated
217 the actual temporal trend. Next, we scanned the data using the Hampel filter function of the 'pracma' R
218 package (Borchers, 2021) with customized moving window length and Pearson's rule threshold value
219 (Pearson, 1999) to flag possible outliers.

220 Despite regular maintenance, many sensors failed to provide data that met the quality criteria during the
221 growing season (March-August) in 2019. Only 56 sensor locations (out of 98) provided data from both
222 top and bottom sensors that met the qualification criteria described above with varying date intervals
223 throughout the growing season. Of these, only 34 sensor locations were used to estimate root water uptake
224 as they simultaneously provided data from both top and bottom sensors within the dry periods.

225 **2.3.2) Soil water calculation**

226 We estimated soil water (S) at measurement locations for the monitored soil layer based on volumetric
227 soil water content measured by top and bottom sensors.

$$228 S_{i,d} = \sum z_t \theta_{i,d}^t + z_b \theta_{i,d}^b \quad (2)$$

229 We similarly integrated the soil water at field capacity ($S_{FC,i}$)

$$230 S_{FC,i} = \sum z_t \theta_{FC,i}^t + z_b \theta_{FC,i}^b \quad (3)$$

231 where z_t is the depth of the soil column monitored by the top sensor and z_b is the depth of soil represented
232 by the bottom sensor, and $\theta_{i,d}$ is volumetric soil water content at location i on date d , and $\theta_{FC,i}$ the soil
233 water content at the field capacity.

234 We calculated bulk density at the sensors' locations for the monitored soil layer.

$$235 \overline{d}_{bulk,i} = \frac{\sum z_t d_{bulk,i}^t + z_b d_{bulk,i}^b}{\sum z_t + z_b} \quad (4)$$

236 where $d_{bulk,i}^t$ and $d_{bulk,i}^b$ are the bulk density of the topsoil and subsoil, respectively, at location i .

237 **2.3.3) Descriptive Statistics**

238 We calculated the coefficient of quartile variation (CQV) and the interquartile range to describe spatial
239 variation of throughfall, volumetric soil water content, and root water uptake. Also, we estimated octile
240 skewness (OS_8) of throughfall based on the first and seventh octile .

$$241 CQV = \frac{Q_3 - Q_1}{Q_3 + Q_1} \quad (5)$$

$$242 OS_8 = \frac{(Q_7 - median) - (median - Q_1)}{Q_7 - Q_1} \quad (6)$$

243 We characterized spatial patterns of daily root water uptake (E_t) by calculating the spatial deviation from
244 the mean ($\delta E_{t,i,d}$, Equation 7) (Vachaud et al., 1985).

$$245 \delta E_{t,i,d} = \frac{E_{t,i,d} - \overline{E_{t,d}}}{\overline{E_{t,d}}} \quad (7)$$

246 where $E_{t,i,d}$ is daily root water uptake estimated at i sensor location on date d and $\overline{E_{t,d}}$ is spatial average
247 of daily root water uptake on date d .

248 Similarly, we calculated the spatial deviation of soil water and throughfall to identify their spatial patterns.

249 **2.4) Root water uptake estimation**

250 We estimated root water uptake using the multi-step, multi-layer regression method (MSML), which is a
251 water-balance method and derives evapotranspiration from diurnal differences in soil water content
252 (Guderle and Hildebrandt, 2015; Guderle et al., 2018). This approach does not require prior information
253 on root structure but relies on high temporal and spatial resolution data on multiple soil layers. Previous
254 studies using additional measurements such as sap-flow and lysimeters demonstrated that the MSML
255 method successfully estimates transpiration in both forest and grassland ecosystems (Guderle et al., 2018;
256 Jackisch et al., 2020).

257 As described in Guderle and Hildebrandt (2015), the MSML derives root water uptake from distinct
258 differences in the day and night portions of soil moisture time series. The main assumption is that, in the
259 absence of rainfall-driven rapid vertical soil water flow, evapotranspiration occurs only during the day,
260 while soil water flow occurs both during the day and at night. As a result, soil moisture time series reflect
261 a distinct day/night signal under dry weather conditions.

262 In applying this method to our study, we first excluded potential periods of fast vertical flow periods from
263 the time series due to previous rainfall events and identified periods for estimating daily root water uptake.
264 We considered an 8 h buffer period to include canopy dripping and 48 h for the cessation of rainfall
265 influence on soil water. Thus, a total of 56 h was the time interval used to define the start of the water
266 uptake estimation period. The period when the root water uptake is estimated is hereafter referred to as
267 the dry period.

268 Next, we split each soil moisture time series into a day (transpiration active period) and a night branch,
269 as explained by Guderle and Hildebrandt (2015). We defined the transpiration period (starts 2 h after
270 sunrise and ends 2 h before sunset) based on local sunrise and sunset time. Sunrise and sunset times were
271 obtained from the R package 'suncal' (Thieurmel and Elmarhraoui, 2022). We fit linear models to each
272 split branch of the time series and derived the slopes. The difference between the slope of the day branch
273 (m_{tot}) and the average slope of the antecedent and preceding night ($\overline{m_{flow,i}}$) gives the rate of water uptake.
274 Thus, we estimated daily evapotranspiration at each soil water content location i (Equation 8, 9) by
275 accounting for soil layer thickness and slope difference-

276

$$277 \quad E_{t,msml,i}^{t,b} = (m_{tot,i}^{t,b} - \overline{m_{flow,t}^{t,b}}) d_{z,i}^{t,b} \quad (8)$$

$$278 \quad E_{t,i} = \sum(E_{t,msml,i}^t + E_{t,msml,i}^b) \quad (9)$$

279

280 **2.5) Linear Mixed Effects Model**

281 We employed a linear mixed effects model to investigate the driving factors for root water uptake patterns.
 282 A linear mixed effects model is a multivariate statistical tool that describes the relationship between a
 283 dependent variable and explanatory variables (fixed effects) while controlling for dependencies in the
 284 data that may arise due to repeated sampling with certain designs (random effects). Fixed effects are
 285 informative, repeatable levels of explanatory and quantified variables that can influence the mean of the
 286 dependent variable, and they can be tested. In addition, in a linear mixed-effects model, how the
 287 relationship between the dependent variable and one predictor depends on the level of another predictor
 288 can be represented via interaction term.

289 Random factors are uninformative levels of predictor variables but can explain parts of the residual of the
 290 fixed effects model by calculating different intercepts for different category levels. They are included in
 291 mixed effects models to account for qualitative information from repeated sampling with respect to
 292 individuals, time stamps, or treatments. Here, sensor location and dry period, i.e. date, are taken as random
 293 effects.

294 For the model, we used only paired throughfall and soil moisture measurement locations where both top
 295 and bottom sensors provided data during the dry periods. All considered explanatory drivers, which are
 296 included as fixed factors in the model, are listed in Table 1. These factors include abiotic and biotic
 297 variables that possibly influence relative local root water uptake: They are daily spatial average soil water
 298 storage, the spatial deviation of soil water from the mean, soil water at field capacity and bulk density of
 299 the monitored soil layer .

300 To account for spatial variability in throughfall, we calculated the spatial deviation from the mean by
 301 using Equation 7. Here we considered this variable at a two-different time scales: the sampling week(s)
 302 prior to root water uptake estimation, and over the entire throughfall sampling period.

303 Further, as biotic factors, we included number of trees, and number of species within a 5 m radius of each
304 soil moisture location, and inverse-distance-weighted basal area (BA) within 5 m radius of each soil
305 moisture location, calculated as follows:

$$306 \quad BA_i = \frac{\sum_{R=1}^R W_R A_{tree}}{A} \quad (10)$$

$$307 \quad \text{with } W_R = \frac{(x_i - x_R)^2}{\sum_R (x_i - x_R)^2} \quad (11)$$

308 where i is the soil moisture sensor located at x_i , R is the tree index located at x_R , and A_{tree} is the individual
309 basal area of the corresponding tree, A is the area around the soil moisture sensor i with 5 m in radius.

310 Even though our research plot is a beech-dominated forest, in some spots, two to four species were present
311 within a 5 m radius of the soil moisture sensors.

312 We also included interaction terms (Table 1) as fixed factors in the model to capture complex and non-
313 linear relationships among the biotic and abiotic factors .

314 We conducted all analyses with the R statistical software (R Core Team, 2022) and used the *lmer* function
315 in the 'lme4' package (Bates et al., 2015) for the model development. We visually checked the model
316 assumptions using the 'check_model' function of the 'performance' package (Lüdtke et al., 2021).

317 In addition, we calculated both conditional and marginal R^2 of the model with the 'MuMIn' package
318 (Bartoń, 2020). While the conditional R^2 includes the variance of the entire model, the marginal R^2
319 subsumes only the fixed effects (Bartoń, 2020). Before fitting the linear mixed effects model, we tested
320 for co-linearity of the considered variables and scaled the data with a Z-transformation by using the 'scale'
321 function in base R (R Core Team, 2022), which allowed us to evaluate the individual effect of fixed effects
322 by comparing slopes and significance levels.

323 We developed the optimal model by applying a systematic model selection procedure based on Akaike's
324 Information Criterion (AIC) comparison in combination with the examination of the factors. Model
325 selection began with the beyond-optimal model, which included all possible fixed and random effects.
326 We stepwise evaluated each fixed effect based on its respective significance (p value comparison) by
327 fitting the model the maximum likelihood (ML) to be able to compare AIC values (Zuur et al., 2009). In
328 each step, starting with interaction terms, we identified the least significant effect and formulated a model
329 without it. We compared the AIC values of the model before and after removing the effect, discarding it

330 in case the AIC was unaffected or decreased. We followed the procedure with the next equally detected
 331 effect, and repeated it until only significant fixed effects remained, and the model with the lowest AIC
 332 (the optimal model) was obtained.

333 As a final step, the best model was refitted with restricted maximum likelihood (REML) (Zuur et al.,
 334 2009).

335 **Table 1** List of fixed and random factors considered for estimating the root water uptake patterns through linear mixed effects
 336 model. Interaction is shown with ‘x’.

Fixed Factors	
Single Factors	Interaction Factors
Spatial average of soil water storage in the monitored soil layer (\bar{S})	$\bar{S} \times S_{FC}$
Spatial deviation of soil water storage from the mean (δS)	$\delta S \times S_{FC}$
Field capacity of the monitored soil layer (S_{FC})	$\delta S \times BA$
Bulk density capacity of the monitored soil layer (d_{bulk})	$\bar{S} \times BA$
Spatial deviation of throughfall of events measured in sampling week previous to the corresponding dry period ($\delta P_{TF_{last\ ev.}}$)	$\delta S \times n_{tree}$
The median of spatial deviation of throughfall measured within the whole sampling period ($\widetilde{\delta P_{TF}}$)	$\bar{S} \times n_{tree}$
Number of trees (n_{tree})	$\delta P_{TF_{last\ ev.}} \times S_{FC}$
Basal area (BA)	$\delta P_{TF_{temp.\ stable.}} \times S_{FC}$
Number of species ($n_{sp,tree}$)	$\delta P_{TF_{last\ ev.}} \times d_{bulk}$
	$\delta P_{TF_{temp.\ stable.}} \times d_{bulk}$
	$n_{sp,tree} \times WA_{int}$
Random factors	
Soil moisture sensor location	
Dry period	

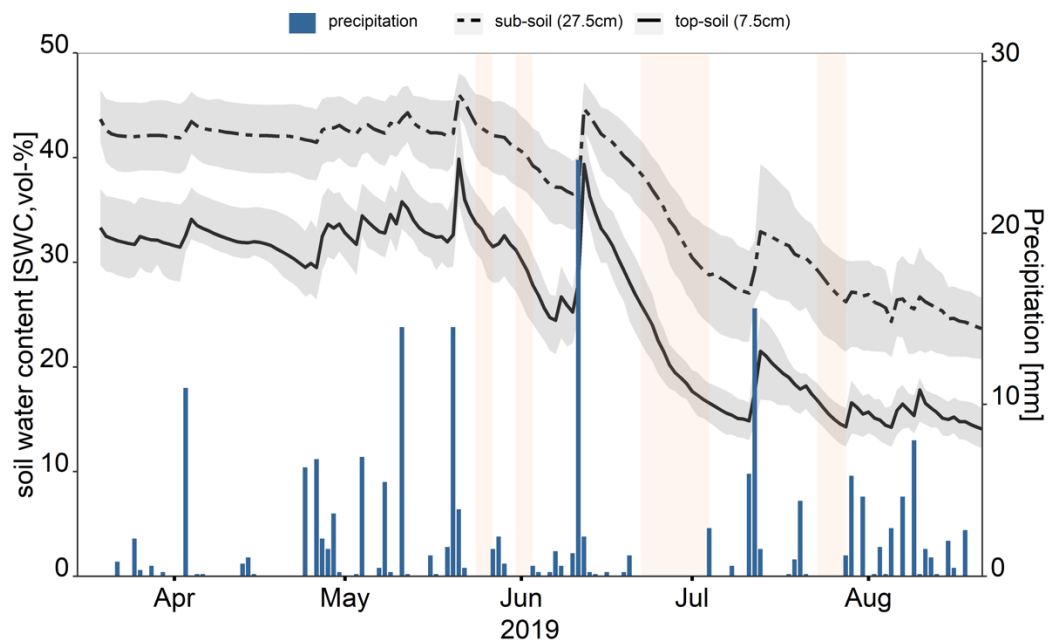
3) Results

3.1) Spatio-temporal distribution of throughfall and soil water content

In 12 out of the 16 sampling weeks, the weekly gross precipitation was more than half of the total potential evapotranspiration. Table 2 shows the distribution of throughfall sampled in 2019 (April-August) at 200 collectors and the 98 collectors that were paired with soil moisture sensors. Weekly throughfall increased with an increase in rain. The coefficient of quartile variation (CQV) of throughfall was generally lower for larger cumulative weekly rains. On average, the collectors paired with soil-moisture sensors received similar amounts of throughfall to all collectors (Table 2). The CQV of data from the paired collectors ranged from 0.27 to 0.6, which is similar to the CQV of throughfall sampled at all collectors. The octile skew (OS_8) of paired and all collectors was also similar.

As the growing season progressed in 2019, the average soil water content decreased in both the topsoil and subsoil. In April and early May, the average volumetric soil water content in the topsoil was above 30%, and dropped to below 10% by the end of August. In the subsoil, the volumetric soil water content similarly declined from above 40 % to below 20 % over the sampling period (Figure 2). On average, soil water changed from 52.5mm to 17.5 mm in the topsoil and from 80 mm to 40mm in the subsoil.

We derived root water uptake for four periods (a total of 19 days) under different soil wetness conditions that captured the seasonal variation of soil water content, including late spring when the soil water content was higher and drier periods during the summer following re-wetted soil conditions with late summer rains. As listed in Table 3 and shown in Figure 2, two periods were in late May and early June, and each lasted two days. The third period began in late June and lasted 11 days; the last was four days in late July. From the start of the first dry period to the end of the last, the average soil water content declined from 33 to 15 % in the topsoil and from 43 to 27% in the subsoil. Table 3 shows that within the dry periods, the coefficient of quartile variation (CQV) of soil water content was between 0.09 -0.14 and 0.08 to 0.16 in the topsoil and subsoil, respectively. During the dry periods, the spatial heterogeneity of soil water content in the subsoil increased systematically. In contrast, the spatial variation of soil water content in the topsoil was not correlated with soil dryness.



363

364

365

366

367

Figure 2 Soil moisture temporal variation in top and subsoil together with the daily precipitation measured at the nearby Reckenbühl station (approximately 1.4 km to the Northeast). The solid and dashed lines are spatial mean of soil water content estimated based on top (7.5 cm) and bottom (27.5 cm) sensors, and grey shaded areas show first and third quartiles. The reddish shaded areas show defined dry periods within the throughfall sampling when root water uptake could be estimated.

Table 2 Cumulative potential evapotranspiration in mm ($E_{\text{pot,cum}}$), gross precipitation (P_g), the ratio of total precipitation to the potential evapotranspiration, spatial mean of throughfall based on all collectors ($\overline{P_{TF}}$), spatial mean of throughfall based paired collectors ($\overline{P_{TF}}$) in mm, interquartile range (IQR), coefficient of quartile variation (CQV) and octile skewness (OS_8) of both all and paired throughfall collectors during the sampling week. The values are ordered according to the cumulated gross precipitation size.

Date	$E_{\text{pot,cum}}$	P_g	P_g/E_{pot}	$\overline{P_{TF}}$	$\frac{IQR}{\overline{P_{TF}}}$	$\frac{CQV}{\overline{P_{TF}}}$	$\frac{OS_8}{\overline{P_{TF}}}$	$\overline{P_{TF,paired}}$	$\frac{IQR}{\overline{P_{TF,paired}}}$	$\frac{CQV}{\overline{P_{TF,paired}}}$	$\frac{OS_8}{\overline{P_{TF,paired}}}$
04-06-2019	13.55	0.76	0.06	0.35	0.18	0.25	0.46	0.34	0.16	0.24	0.49
26-06-2019	20.87	1.73	0.08	0.97	0.44	0.24	0.16	0.98	0.53	0.27	0.27
17-04-2019	5.62	2.42	0.43	1.72	0.27	0.08	0.23	1.72	0.33	0.09	0.09
18-06-2019	9.46	4.00	0.42	2.58	0.62	0.12	-0.03	2.57	0.53	0.10	-0.08
29-05-2019	10.15	6.27	0.62	3.77	1.24	0.17	-0.52	3.63	1.50	0.21	-0.42
24-07-2019	13.52	7.80	0.58	4.61	1.06	0.12	-0.34	4.48	0.88	0.10	-0.63
21-08-2019	8.94	8.54	0.96	5.19	1.06	0.10	-0.47	5.17	0.97	0.10	-0.44
30-07-2019	12.68	10.73	0.85	7.81	2.25	0.15	-1.51	7.58	2.28	0.15	-1.17
07-05-2019	6.65	12.56	1.89	9.21	1.33	0.07	-0.75	9.21	1.99	0.11	-1.05
14-08-2019	8.51	13.79	1.62	11.19	2.65	0.12	-1.40	10.99	2.98	0.13	-1.13
08-08-2019	13.91	23.87	1.72	16.60	2.65	0.08	-1.10	16.52	2.65	0.08	-1.17
30-04-2019	5.93	24.47	4.13	18.44	3.09	0.08	-1.63	18.30	2.65	0.07	-1.23
17-07-2019	8.28	29.27	3.54	24.22	3.54	0.07	-2.08	24.39	3.54	0.07	-2.59
15-05-2019	7.42	29.53	3.98	22.10	3.54	0.08	-2.11	22.21	3.54	0.08	-2.11
22-05-2019	6.74	41.82	6.20	30.94	3.54	0.06	-3.04	30.54	3.54	0.06	-3.46
13-06-2019	14.47	71.84	4.96	57.77	8.51	0.07	-5.82	57.99	7.29	0.06	-6.52

369 **Table 3** The spatial average of daily volumetric soil water content ($\overline{\theta_{\text{top-soil}}}$, vol-%) in topsoil (0-17.5 cm), and ($\overline{\theta_{\text{subsoil}}}$, vol-%)
 370 in subsoil (17.5 – 37.5 cm) during the defined dry periods. The inter quartile range (IQR), and coefficient of quartile variation
 371 (CQV) of daily volumetric soil water content in both layers during the dry periods.

Date	$\overline{\theta_{\text{top-soil}}}$ (vol-%)	IQR $\theta_{\text{top-soil}}$ (vol-%)	CQV $\theta_{\text{top-soil}}$ (vol-%)	$\overline{\theta_{\text{sub-soil}}}$ (vol-%)	IQR θ_{subsoil} (vol-%)	CQV θ_{subsoil} (vol-%)	Dry Period
25-05-2019	33.17	5.72	0.09	42.82	6.72	0.08	1
26-05-2019	32.12	6.62	0.10	42.46	6.67	0.08	1
01-06-2019	30.23	6.87	0.12	40.61	6.9	0.09	2
02-06-2019	29.22	7.23	0.13	40.11	6.85	0.09	2
23-06-2019	25.01	6.69	0.14	37.80	6.38	0.08	3
24-06-2019	24.04	6.45	0.14	36.94	6.22	0.08	3
25-06-2019	22.52	5.43	0.12	36.13	6.54	0.09	3
26-06-2019	21.48	5.07	0.12	35.24	6.71	0.10	3
27-06-2019	20.20	4.25	0.11	33.98	7.75	0.12	3
28-06-2019	19.45	3.85	0.10	33.31	8.08	0.12	3
29-06-2019	18.98	3.83	0.10	32.36	8.05	0.12	3
30-06-2019	18.44	3.52	0.09	31.37	8.15	0.13	3
01-07-2019	17.67	3.62	0.10	30.45	8.18	0.13	3
02-07-2019	17.29	4.18	0.12	29.84	8.87	0.15	3
03-07-2019	16.89	3.72	0.11	29.26	8.98	0.15	3
24-07-2019	16.15	3.48	0.11	28.56	8.7	0.16	4
25-07-2019	15.51	3.47	0.11	27.85	8.67	0.16	4
26-07-2019	14.98	3.57	0.12	27.21	8.49	0.16	4
27-07-2019	14.57	3.65	0.13	26.65	8.63	0.16	4

372

373 **3.2) Soil water storage, potential evapotranspiration, and root water uptake**

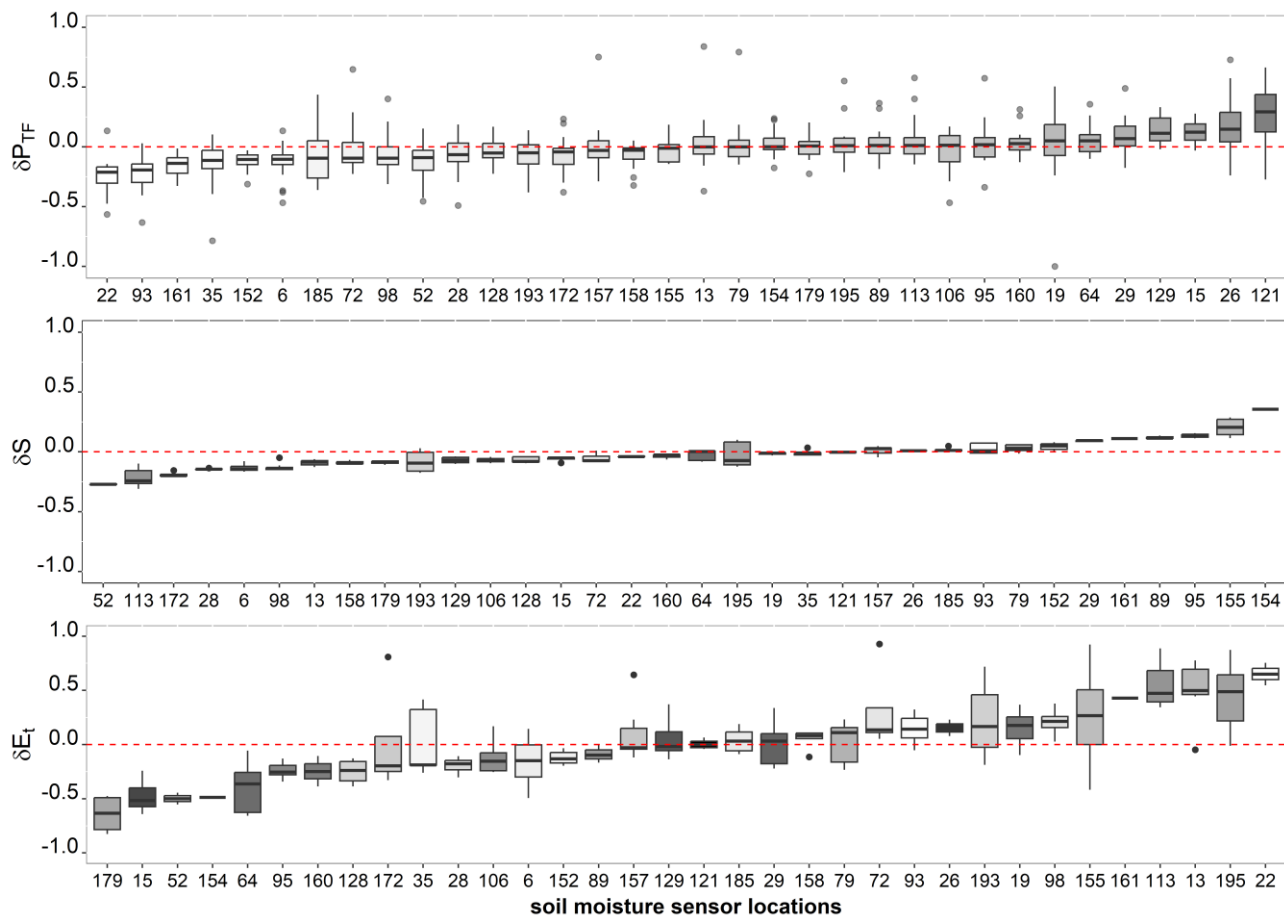
374 The integrated field capacity of the monitored soil depth was 160 mm on average at the research site.
 375 Table 4 shows that soil water was much lower than the field capacity during the dry periods, and the
 376 mean soil water storage dropped below 42 mm in late July. In addition, Table 4 demonstrates that the
 377 average root water uptake (\overline{E}_t) ranged from 0.94 mm d⁻¹ to 3 mm d⁻¹ while potential evapotranspiration
 378 (E_{pot}) ranged from 1.75 mm d⁻¹ to 3.12 mm d⁻¹. The discrepancy between average root water uptake and
 379 the potential evapotranspiration increased as soil water decreased, especially during the longest dry period
 380 (Table 4). Root water uptake showed greater spatial variation than water input and soil wetness. The
 381 coefficient of quartile variation (CQV) of root water uptake ranged from 0.15 to 0.28, which was higher
 382 than the CQV of throughfall and volumetric soil water content in both soil layers.

383 **Table 4** The daily average air temperature (T_{air} , °C), potential evapotranspiration (E_{pot} , mm), mean soil water storage (\bar{S} , mm)
 384 in monitored soil layer (0 - 37.5 cm), and spatial mean of daily root water uptake (\bar{E}_t , mm) based on all soil moisture sensors,
 385 and the ratio of the root water uptake to the potential evapotranspiration together with and standard deviation (SD) and
 386 coefficient of quartile variation (CQV) of the daily root water uptake during the defined dry periods

Date	T_{air} (°C)	E_{pot} (mm)	\bar{S} (mm)	\bar{E}_t (mm)	$\bar{E}_t / E_{\text{pot}}$ (%)	SD \bar{E}_t	CQV \bar{E}_t	Dry Period
25-05-2019	12.74	1.80	71.94	1.09	60.56	0.38	0.28	1
26-05-2019	14.43	1.90	70.57	1.30	68.42	0.48	0.25	1
01-06-2019	18.42	2.59	67.16	2.26	87.26	0.98	0.27	2
02-06-2019	21.38	2.77	65.79	2.50	90.25	1.12	0.18	2
23-06-2019	19.45	2.79	59.81	2.83	101.43	0.90	0.19	3
24-06-2019	20.22	2.82	58.16	2.62	92.91	0.76	0.17	3
25-06-2019	22.52	2.89	55.96	2.67	92.39	0.78	0.16	3
26-06-2019	25.73	2.96	54.13	3.00	101.35	0.88	0.15	3
27-06-2019	18.83	2.75	51.91	2.28	82.91	0.55	0.16	3
28-06-2019	16.07	2.58	50.55	1.53	59.30	0.40	0.20	3
29-06-2019	19.59	2.85	49.55	2.11	74.04	0.60	0.20	3
30-06-2019	25.54	3.12	48.26	2.57	82.37	0.86	0.18	3
01-07-2019	20.63	2.30	46.69	1.59	69.13	0.53	0.18	3
02-07-2019	14.88	1.75	45.81	1.08	61.71	0.42	0.24	3
03-07-2019	13.77	1.91	44.95	0.94	49.21	0.30	0.23	3
24-07-2019	24.39	2.76	43.61	1.88	68.12	0.64	0.19	4
25-07-2019	25.33	2.82	42.31	1.77	62.77	0.60	0.24	4
2019-07-26	23.27	2.64	41.18	1.40	53.03	0.55	0.18	4
2019-07-27	21.29	2.68	40.23	1.21	45.15	0.47	0.19	4

387 3.3) Soil water, throughfall, and root water uptake patterns

388 At soil moisture measurement points where daily root water uptake was determined ($n = 34$), we
 389 calculated the spatial deviation from the median of throughfall, soil water storage, and root water uptake
 390 to illustrate the spatial patterns. Figure 3 shows that some locations received repeatedly less (or more)
 391 throughfall than average ($\delta P_{TF} < 0$), some locations were repeatedly wetter or drier ($\delta S < 0$), and some
 392 places regularly had lower or higher root water uptake (δE_t) throughout the sampling period. However,
 393 these locations were not related to each other. In fact, Figure 3 demonstrates that neither throughfall nor
 394 soil water patterns are directly correlated with the root water uptake patterns. For example, the locations
 395 with higher water uptake were not coupled with elevated throughfall input (locations colored dark) or
 396 higher soil water storage. In addition, soil water storage patterns were not correlated with throughfall
 397 patterns.



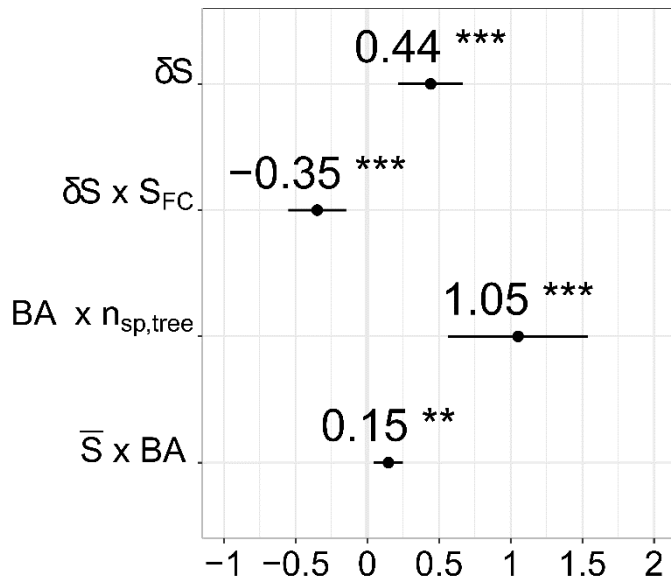
398

399 **Figure 3** Temporal stability of throughfall patterns which is estimated by the spatial deviation from the mean (δP_{TF}) throughout
 400 the sampling period in 2019 (April-August), soil water (δS) and root water uptake (δE_r) based on the spatial deviation from
 401 the mean during the defined dry periods. Soil moisture sensor locations colored according to throughfall input.

402 **3.5) Fixed factors regulating root water uptake patterns**

403 We used a linear mixed effects model to disentangle the effects of throughfall, soil water, soil properties,
 404 and the neighbouring tree characteristics on root water uptake patterns. The fixed and random effects
 405 contributed almost equally to the model. The R^2 of the model was 0.77, and the contribution of the fixed
 406 effect to the R^2 was 0.39 (See the supplement for more details on the optimal model).

407 Figure 4 shows only the significant fixed effects for root water uptake patterns. Spatial deviation of soil
 408 water from the mean (i.e., soil water patterns) was the only single and the most significant factor positively
 409 related to the spatial deviation of root water uptake. Thus, water uptake was elevated at locations where
 410 the most water was retained in the soil at the given time, i.e., greater soil water storage.

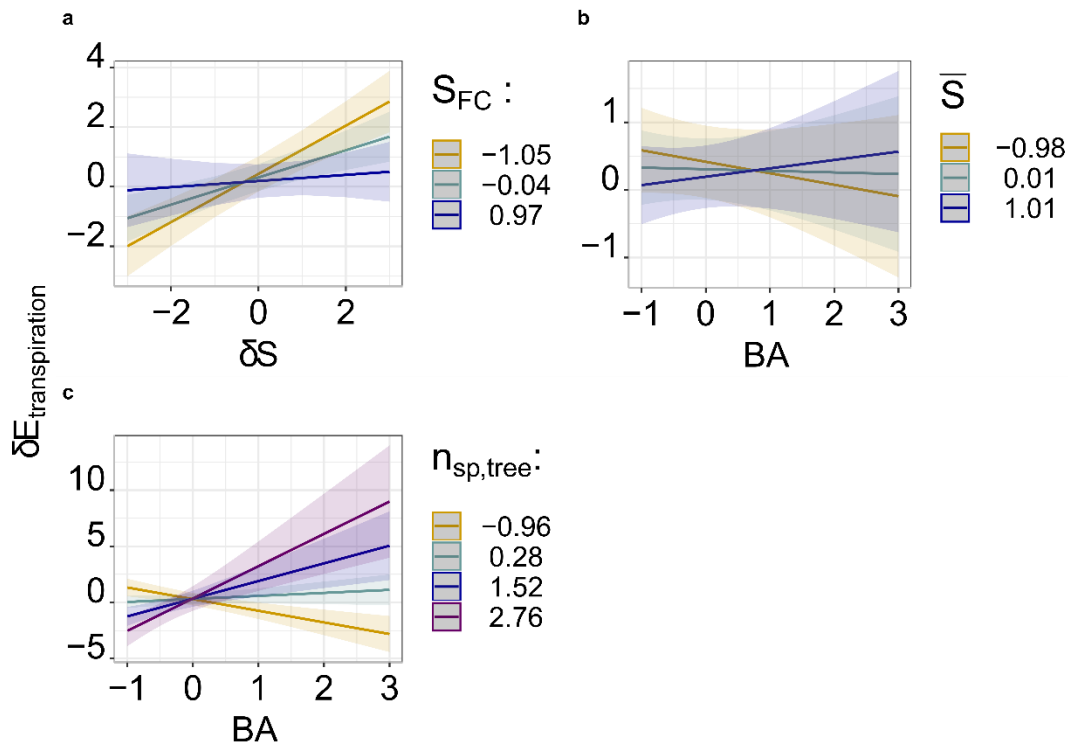


411

412 **Figure 4** The significant fixed factors of the best model to estimate root water uptake patterns (δE_i). Values on the x-axis
 413 indicate the slope of the relations. All variables were scaled by Z-transformation. Interaction is shown with 'x'. Here δS is the
 414 spatial deviation of soil water, S_{FC} is the field capacity, $n_{sp,tree}$ is the number of species, BA is the basal area, and \bar{S} is soil water
 415 storage. Significance codes are *** $\cong 0$, ** $\cong 0.001$. (the details on the model can be found in the supplement)

416 Field capacity by itself was not a significant factor affecting local root water uptake. However, it strongly
 417 influenced how local soil water controlled root water uptake as a part of the significant interaction term.
 418 Figure 5a illustrates how to root water uptake was more dependent on local soil water when field capacity
 419 was low (i.e., higher macroporosity). In contrast, soil bulk density and therefore total porosity was not
 420 part of the final model.

421 Although the spatial average of soil water storage, e.g., the state of wetness, was not an important factor
 422 for local root water uptake by itself, it moderated the impact of basal area (BA) on the spatial distribution
 423 of water uptake. We found that as the plot dries, uptake shifts from places with higher to places with lower
 424 basal area (Figure 5b). Furthermore, the statistical model revealed that water uptake increased with the
 425 higher basal area at locations where multiple species co-existed (Figure 5c). However, the number of
 426 species and the basal area were individually not significant fixed effects. Lastly, throughfall patterns were
 427 not significant predictors of local root water uptake. Only the median of the spatial deviation of
 428 throughfall, which represents temporally stable patterns within the sampling period ($\widetilde{\delta P_{TF}}$), marginally
 429 improved the final model.



430

431 **Figure 5** Visualisation of the significant relations shown in Figure 4, representing the significant drivers of root water uptake
 432 patterns during the defined dry periods. Relation to (a) interactive relation of the spatial deviation of soil water storage and
 433 field capacity (S_{FC}), (b) the interactive relation of basal area (BA) and the spatial average of soil water storage (\bar{S}), (c) the
 434 interactive relation of number of species ($n_{sp,tree}$) and basal area (BA).

435 **4) Discussion**

436 We investigated the role of throughfall, soil water patterns, and soil and tree characteristics on the spatial
 437 variation of root water uptake. In the following sections we discuss three main findings, which are: (1)
 438 Contrary to our hypothesis, throughfall patterns do not play a role not in root water uptake patterns despite
 439 the recurrence of distinctly localized greater and lesser throughfall inputs. (2) How and where water is
 440 stored in the soil, which is strongly determined by soil hydraulic properties, dominates water uptake
 441 patterns. (3) The size and species of neighbouring trees regulate relative local water uptake such that
 442 locations surrounded by more diverse neighbourhoods are subject to greater water uptake.

443 **4.1) Spatial variation in throughfall does not affect root water uptake patterns**

444 We adequately captured the spatial distribution and temporal stability of throughfall at locations where
445 local root water uptake was derived. Consistent with previous observations in temperate forests (e.g.,
446 Whelan and Anderson, 1996; Staelens et al., 2006; Metzger et al., 2017), the amount of weekly rainfall
447 significantly altered the spatial distribution of throughfall such that more rainfall, and thus more
448 throughfall, resulted in less spatial variability. Previous studies repeatedly showed that throughfall
449 patterns exhibit temporal stability in forest ecosystems (e.g., Keim et al., 2005; Staelens et al., 2006;
450 Wullaert et al., 2009; Rodrigues et al., 2022). At our research site, using event-based sampling, Metzger
451 et al., (2017) and Fischer-Bedtke et al., (2023) demonstrated that throughfall patterns persist over time,
452 which was also true for our weekly sampling in 2019. With canopy cover being the key driver of
453 throughfall (Fischer-Bedtke et al., 2023), it is not surprising that weekly cumulative events resulted in a
454 localized high and low throughfall input.

455 Contrary to expectations (Bouten et al., 1992; Guswa and Spence, 2012; Coenders-Gerrits et al., 2013;
456 Fischer-Bedtke et al., 2023), our results showed that throughfall hotspots do not increase or facilitate
457 greater root water uptake. In addition, the linear mixed effects model results confirmed that throughfall
458 patterns do not drive the variation in root water uptake. We attributed the absence of this to two reasons:
459 (1) decoupled soil water and throughfall patterns, (2) non-water limited conditions.

460 Regarding (1), we confirmed that the temporally stable throughfall patterns do not correspond to the post-
461 event soil water and root water uptake patterns. We paired the measurements of throughfall and soil water
462 content measurements – and thus the estimates of root water uptake- within a distance of 1 m. The spatial
463 correlation length of soil water content and throughfall is on the order of 6-10 m in natural temperate
464 forests (Keim et al., 2005; Gerrits et al., 2010; Zehe et al., 2010). In the same study site with the spatially
465 extended throughfall sampling, Fischer-Bedtke et al., (2023) found that the throughfall correlation length
466 increased with decreasing event size, varying from 6.2 m to 9.5 m depending on the size of the rain events.
467 Thus, the paired sampling design in our study likely provided co-located throughfall and soil moisture
468 measurements. However, variation in soil water storage was not related to throughfall patterns despite
469 temporally persistent local high and low throughfall inputs.

470 Some studies, mostly conducted in the arid regions and coniferous forests, reported that soil wetting
471 patterns were not or only partly linked to throughfall variation, despite recurrent throughfall patterns (Raat
472 et al., 2002; Shachnovich et al., 2008; Zhu et al., 2021). Forest floor thickness, horizontal water flow, and
473 soil properties were suggested as reasons for the decoupled patterns. Other modelling and field studies
474 conducted in temperate deciduous forests found that throughfall patterns influenced soil moisture
475 response to rain event rather than post-event soil water storage variability (Coenders-Gerrits et al., 2013;
476 Metzger et al., 2017; Fischer et al., 2023). These studies attributed possible reasons to local processes
477 such as preferential flow due to soil water repellency, the soil pore structure, or elevated root water uptake.
478 Our results support that it is not root water uptake but preferential flow paths that are likely to decouple
479 the throughfall and soil water patterns. In fact, Fischer-Bedtke et al., (2023) using independent throughfall
480 and soil water content sampling designs, demonstrated that the signature of throughfall patterns dissipated
481 in the post-event soil water variation. However, they detected the stronger influence of throughfall
482 patterns in the soil moisture response to rainfall in the 2015 and 2016 growing seasons. The temporal
483 variation in soil water content in the 2019 growing season was similar to the seasonal decline in soil water
484 content in 2015 (Metzger et al., 2017). Dry soil conditions can lead to rapid drainage due to reduced water
485 holding capability (Jost et al., 2004; Blume et al., 2009; Wiekenkamp et al., 2016; Demand et al., 2019;
486 Molina et al., 2019) regardless of throughfall amount and its variation. Therefore, our findings support
487 that the localized throughfall input potentially enhances preferential flow because of low soil retention
488 (Fischer-Bedtke et al., 2023) rather than local root water uptake. As a result, the fast flow processes likely
489 dominate how water is stored and transported at our site, erasing the throughfall distribution signature in
490 soil water and root water uptake patterns. Moreover, any short-term response of uptake to throughfall
491 could not be captured as water uptake was calculated only after 56 hours had elapsed since the last rain
492 event, yet we showed that temporally stable hotspots are not associated with elevated water uptake.
493 Hence, our results are consistent with previous propositions stating that the spatial variation of throughfall
494 affects drainage and subsurface flow (Keim et al., 2006; Blume et al., 2009; Guswa and Spence, 2012),
495 while root activities such as water uptake and hydraulic redistribution do not alter canopy-attributed
496 heterogeneity in drainage pathways (Guswa, 2012).

497 The second reason (2) is related to water-limitation conditions. In central Europe, 2019 was the second
498 consecutive extremely dry summer (Boergens et al., 2020), which damaged beech forests (Obladen et al.,
499 2021). On average, however, the potential evapotranspiration demand was met at the study site despite
500 the low soil water storage. The ratio of root water uptake to potential evapotranspiration was mostly above
501 65%, which is within the expected range even in the absence of shallow groundwater storage (Nie et al.,
502 2021). Hence, local biotic and soil tied abiotic factors determined the spatial variation of root water uptake
503 during growing season rather than throughfall -water input- patterns. However, the discrepancy between
504 daily potential evapotranspiration and root water uptake only increased as the soil in the sampled layers
505 dried out, due to a potential shift in the water uptake depth (see below).

506 **4. 2) Relative and average soil wetness shapes root water uptake patterns**

507 We found that spatial variation in soil water storage strongly regulates local water uptake such that wetter
508 locations enhance root water uptake. This finding is consistent with expectations as transpiration rate
509 relies on soil water availability and distribution (Couvreur et al., 2014; Klein et al., 2014; Hildebrandt et
510 al., 2016). Here, we provide further support that root water uptake is likely to reduce the spatial variability
511 in soil water storage as has been previously suggested (Hopmans and Bristow, 2002; Ivanov et al., 2010;
512 Neumann and Cardon, 2012).

513 Trees take up more water in locations where water is not subject to throughfall-driven rapid drainage (see
514 above), as a result root water uptake patterns are determined by where water is retained longer in the soil.
515 Our results support previous studies suggesting that tree transpiration demand is met by water with longer
516 residence time in the soil matrix - passive storage - while groundwater recharge is fed by rapid flow -
517 active storage (e.g, Evaristo et al., 2019; Sprenger et al., 2019). In our statistical analyses, we investigated
518 the soil properties of bulk density and field capacity, which are strongly dependent on other soil properties
519 that control aggregation and soil structure. Although bulk density is strongly related to texture, porosity,
520 soil organic carbon content , , all of which also affect water retention (Zacharias and Wessolek, 2007;
521 Looy et al., 2017), surprisingly soil bulk density was not retained as a predictive variable in the optimal
522 model. .In contrast, the interaction term including field capacity and local soil water storage was
523 significant in the model with a negative relationship with relative water uptake, showing that the

524 combination of higher field capacity (fewer macropores) and low soil water hinders water uptake because
525 water more is more strongly bound in the soil. Differences in local soil properties regulate the matric
526 potential at a certain soil wetness. Thus, wetter locations do not necessarily correspond to those of easier
527 root water uptake due to differences in the soil water retention characteristics (Vereecken et al., 2007; Cai
528 et al., 2018) for which field capacity serves as a proxy. However soil properties alone were less important
529 (smaller effects size of the interaction term including field capacity) than other factors despite their control
530 on the spatial distribution of soil moisture (Vereecken et al., 2022). .

531 In addition, the spatial mean of soil water - a measure of overall wetness of the stand - influenced root
532 water uptake patterns, yet the effect depended on the basal area of neighboring trees. We found that as
533 the study site dries out, local water uptake increased in locations with smaller basal areas. Conversely,
534 wetter site conditions facilitate greater water uptake at locations with higher basal areas, i.e., dense
535 clusters of large trees. We interpret this as a sign that larger trees are likely to shift their water uptake to
536 deeper soil layers to meet transpiration demands, beyond the monitored soil depth (37 cm), as follows:

537 Higher basal area is likely to increase transpiration demand and enhance water uptake as long as water is
538 available. Moreover, locations with higher basal area exhaust the water storage more rapidly as these
539 locations host larger root structure and root biomass (Le Goff and Ottorini, 2001). At the same time, larger
540 sized trees can shift uptake to deeper layers (Gaines et al., 2016).

541 Beech trees have extensive root systems at shallower depths similar to other temperate tree species, such
542 as European ash and sycamore maple (Kreuzwieser and Gessler, 2010; Brinkmann et al., 2019) Despite
543 their shallower root system (Leuschner, 2020) in response to declining soil water content in the topsoil,
544 temperate tree species can tap water from the deeper soil layers (Brinkmann et al., 2019; Agee et al.,
545 2021; Seeger and Weiler, 2021) Recently, Agee et al. (2021) used a three-dimensional water uptake model
546 based on observations in temperate mixed-deciduous forest to show that water uptake is shifted to the
547 deeper soil layers as soil moisture depletes, which is consistent with the field observations. Moreover,
548 Krämer and Hölscher (2010) observed in beech and mixed deciduous stands that roots can extract water
549 at depths down to 70 cm soil depth. Similar to our site, theirs had a shallow soil layer underlain by
550 weathered limestone, but the soil depth varied between 50 and 120 cm. Brinkmann et al., (2019) also

551 observed similar depth range for beech-trees in a mixed forest by tracing stable water isotopes of soil and
552 xylem water.

553 Further tree age and size can affect both individual and stand level transpiration because of the different
554 physiological characteristics and biometrics of trees associated with them (Kostner et al., 2002; Tsuruta
555 et al., 2023). Within the same species, the larger -presumably older- trees have an advantage in accessing
556 the deeper water storages because of their larger root biomass (Le Goff and Ottorini, 2001) and root
557 plasticity may be able to shift the depth of water uptake while younger trees rely on shallower soil water
558 storages (Dawson, 1996). Our results can be interpreted as tree size, which can be attributed to tree age,
559 affecting root water uptake patterns through differential root biomass development. Furthermore, in the
560 Hainich the coexisting species most likely represent highly coherent rooting depth distribution among
561 trees (Gebauer et al., 2012; Meinen et al., 2009) yet adopt different water uptake strategies (see below).
562 Hence consistent with previous studies focusing on temperate tree species, the linear mixed effect model
563 results indicate that trees of different sizes response to declining soil water content by shifting water
564 uptake depth.

565 **4.3) Tree species richness regulates root water uptake patterns**

566 In addition to the basal area, we included the number of species and number of tree individuals in the
567 linear mixed effects analysis to further explore the biotic drivers of root water uptake patterns. While the
568 number of trees was unimportant, the number of species and the basal area showed a significant
569 interaction effect on the local water uptake. The result indicates that an increase in species richness leads
570 to greater root water uptake, depending on the size and/or density of the neighboring trees: Higher basal
571 area, combined with more species, elevates water uptake. In other words, the interactions among
572 neighboring tree species strongly determine root water uptake patterns, and for the same basal area, more
573 water can be taken up in a diverse neighborhood than in a less diverse locations.

574 In temperate forests, transpiration has been observed to change with tree species richness at the stand
575 level (Krämer and Hölscher, 2010; Gebauer et al., 2012; Kunert et al., 2012; Meißner et al., 2012;
576 Forrester, 2014). Although some studies indicate a positive relationship between tree diversity and water
577 uptake rate (Forrester et al., 2010; Krämer and Hölscher, 2010; Kunert et al., 2012), tree species diversity

578 is not always positively related to water uptake. While Krämer and Hölscher (2010) observed a positive
579 correlation between water uptake and species richness of the plots in the upper soil layers during soil
580 drying in 2006 at the same study site, Meißner et al. (2012) found no relationship between tree diversity
581 and root water uptake in 2009. They attributed this finding to wetter soil conditions. In contrast, Lübbe et
582 al. (2016) observed a weak effect of diversity on transpiration in wetter soil conditions but not in drier
583 conditions compared to previous studies (e.g., Pretzsch et al., 2013; del Río et al., 2014). Shortage of
584 water can inflate competition mechanisms for water among tree species (González de Andrés et al., 2018;
585 Vitali et al., 2018; Magh et al., 2020). Our results indicate that competition between neighboring tree
586 species increases water uptake capacity at more diverse spots (Wambsganss et al., 2021).

587 In addition, different co-existing tree species can facilitate resource uptake or reduce competition,
588 depending on the temporal and spatial availability of the sources, which is often defined as
589 complementarity (Forrester and Bauhus, 2016). As reviewed and listed by Silvertown et al. (2015),
590 several studies suggest that co-existing tree species reduce competition for subsurface water sources by
591 adopting different vertical root water uptake strategies, referred to as hydrological niche partitioning. In
592 addition, trees can transport water from wet to dry parts of the soil layers through their roots (Neumann
593 and Cardon, 2012). The mechanism is called hydraulic redistribution or hydraulic lift, which can provide
594 water availability to the shallow roots in drier layers (Burgess et al., 1998; Jonard et al., 2011; Hafner et
595 al., 2017; Lee et al., 2018; Rodríguez-Robles et al., 2020; Hafner et al., 2021). In an experiment with six
596 temperate tree species, including the European beech, Hafner et al. (2021) found that the neighboring tree
597 species diversity may not be important for exploiting water uptake through hydraulic redistribution. Both
598 hydraulic niche partitioning and redistribution have been observed vertically, whereas horizontal patterns
599 are largely unexplored the context of niche partitioning (Hildebrandt, 2020). Our results do not provide
600 direct evidence for either hydraulic redistribution or horizontal niche partitioning. However, they indicate
601 that horizontal root water uptake patterns are regulated by species richness and interactions among
602 neighbouring trees. Thus, we emphasize here the complex interplay between tree species diversity,
603 complementary mechanisms, and water uptake patterns, which is consistent not only with the above-
604 mentioned plot-scale studies, but also with larger-scale studies. For instance Knighton et al., (2019) using
605 the Budyko framework across more than one hundred catchments found that transpiration losses in

606 catchments with deep rooted and mixed species forests differed from those in monoculture catchments.
607 In other words, both plot and catchment scale studies support our results showing that interactions among
608 different coexisting species play a significant role in the spatio-temporal variation of root water uptake.

609 **5) Conclusion**

610 We investigated the factors that influence the spatial patterns of root water uptake by considering
611 heterogeneity in throughfall and soil water. To that end, we acquired a comprehensive data set based on
612 throughfall measurements paired with soil moisture sensors in a mixed deciduous forest. Soil and
613 neighboring tree characteristics were also included in the linear mixed effects model. We found that
614 variation in root water uptake did not correspond to throughfall consequently rejecting our hypothesis
615 that variation in throughfall is imprinted in water uptake patterns. Wetter soil locations, also poorly
616 associated with higher throughfall, increased local root water uptake. In contrast, how average soil water
617 conditions modified root water uptake depended on the neighborhood basal area. As the site dried out,
618 large trees likely took up water in deeper layers to meet transpiration demands. Furthermore, an increase
619 in species diversity promoted root water uptake, similarly depending on the size of neighboring trees,
620 suggesting active complementarity mechanisms in the forest stand. In conclusion, our results manifest
621 that soil water distribution and neighboring tree characteristics regulate root water uptake patterns more
622 than soil properties and throughfall variation.

623

624 **Acknowledgments**

625 This study is part of the Collaborative Research Centre (CRC 1076 AquaDiva) of the Friedrich Schiller
626 University Jena, funded by the Deutsche Forschungsgemeinschaft (DFG, German Research
627 Foundation)—SFB 1076—Project Number 218627073. We thank to AquaDiva subproject D03 for
628 weather station (Reckenbuel) data. Also, people who contributed to installation of soil moisture sensors
629 in the research site: Ricardo Ontiveros-Enriques, Bernd Ruppe, Danny Schelhorn, Josef Weckmüller. We
630 thank the Hainich CZE site manager Robert Lehmann and the Hainich National Park. We thank the

631 bachelor and master students Carla Peter, Xiaoyu Zhao, Stephan Bock for their contribution to throughfall
632 sampling.

633

634 **Data availability**

635 The dataset is currently being prepared for publication in an official repository. The DOI will be published
636 with the data at the latest when the data are published.

637

638 **Author contributions**

639 GD and AH designed the throughfall measurement setup, AH and JCM designed soil moisture
640 measurement. GD conducted the field sampling with assistance from JF and the students listed in the
641 Acknowledgments. GD analyzed the data, developed the linear mixed effects model, and analyzed the
642 results with AH and AG. GD prepared the first version of the manuscript, and all authors contributed to
643 discussions and the final version of the manuscript.

644 **Competing interests**

645 Anke Hildebrandt is part of the editorial board of HESS. The peer-review process was guided by an
646 independent editor, and the authors have also no other competing interests to declare.

647

648 **6) References**

649 Agee, E., He, L., Bisht, G., Couvreur, V., Shahbaz, P., Meunier, F., Gough, C. M., Matheny, A. M.,
650 Bohrer, G., and Ivanov, V.: Root lateral interactions drive water uptake patterns under water limitation,
651 *Advances in Water Resources*, 151, 103896, <https://doi.org/10.1016/j.advwatres.2021.103896>, 2021.

652 Bachmair, S., Weiler, M., and Troch, P. A.: Intercomparing hillslope hydrological dynamics: Spatio-
653 temporal variability and vegetation cover effects, *Water Resources Research*, 48,
654 <https://doi.org/10.1029/2011WR011196>, 2012.

655 Baroni, G., Ortuani, B., Facchi, A., and Gandolfi, C.: The role of vegetation and soil properties on the
656 spatio-temporal variability of the surface soil moisture in a maize-cropped field, *Journal of Hydrology*,
657 489, 148–159, <https://doi.org/10.1016/j.jhydrol.2013.03.007>, 2013.

658 Bartoń, K.: MuMIn: Multi-Model Inference, 2020.

- 659 Bates, D., Mächler, M., Bolker, B., and Walker, S.: Fitting Linear Mixed-Effects Models Using **lme4**, J.
660 Stat. Soft., 67, <https://doi.org/10.18637/jss.v067.i01>, 2015.
- 661 Blume, T., Zehe, E., and Bronstert, A.: Use of soil moisture dynamics and patterns at different spatio-
662 temporal scales for the investigation of subsurface flow processes, *Hydrology and Earth System Sciences*,
663 13, 1215–1233, <https://doi.org/10.5194/hess-13-1215-2009>, 2009.
- 664 Boergens, E., Güntner, A., Dobslaw, H., and Dahle, C.: Quantifying the Central European Droughts in
665 2018 and 2019 With GRACE Follow-On, *Geophysical Research Letters*, 47, e2020GL087285,
666 <https://doi.org/10.1029/2020GL087285>, 2020.
- 667 Bogena, H. R., Herbst, M., Huisman, J. A., Rosenbaum, U., Weuthen, A., and Vereecken, H.: Potential
668 of Wireless Sensor Networks for Measuring Soil Water Content Variability, *Vadose Zone Journal*, 9,
669 1002–1013, <https://doi.org/10.2136/vzj2009.0173>, 2010.
- 670 Borchers, H. W.: *pracma: Practical Numerical Math Functions*, 2021.
- 671 Bouten, W., Heimovaara, T. J., and Tiktak, A.: Spatial patterns of throughfall and soil water dynamics in
672 a Douglas fir stand, *Water Resources Research*, 28, 3227–3233, <https://doi.org/10.1029/92WR01764>,
673 1992.
- 674 Brinkmann, N., Eugster, W., Buchmann, N., and Kahmen, A.: Species-specific differences in water
675 uptake depth of mature temperate trees vary with water availability in the soil, *Plant Biology*, 21, 71–81,
676 <https://doi.org/10.1111/plb.12907>, 2019.
- 677 Brum, M., Vadeboncoeur, M. A., Ivanov, V., Asbjornsen, H., Saleska, S., Alves, L. F., Penha, D., Dias,
678 J. D., Araújo, L. E. O. C., Barros, F., Bittencourt, P., Pereira, L., and Oliveira, R. S.: Hydrological niche
679 segregation defines forest structure and drought tolerance strategies in a seasonal Amazon forest, *Journal*
680 *of Ecology*, 107, 318–333, <https://doi.org/10.1111/1365-2745.13022>, 2019.
- 681 Burgess, S. S. O., Adams, M. A., Turner, N. C., and Ong, C. K.: The redistribution of soil water by tree
682 root systems, *Oecologia*, 115, 306–311, <https://doi.org/10.1007/s004420050521>, 1998.
- 683 Cai, G., Vanderborght, J., Langensiepen, M., Schnepf, A., Hüging, H., and Vereecken, H.: Root growth,
684 water uptake, and sap flow of winter wheat in response to different soil water conditions, *Hydrol. Earth*
685 *Syst. Sci.*, 22, 2449–2470, <https://doi.org/10.5194/hess-22-2449-2018>, 2018.
- 686 Cardon, G. E. and Letey, J.: Plant Water Uptake Terms Evaluated for Soil Water and Solute Movement
687 Models, *Soil Science Society of America Journal*, 56, 1876–1880,
688 <https://doi.org/10.2136/sssaj1992.03615995005600060038x>, 1992.

- 689 Carlyle-Moses, Darryl. E., Lishman, Chad. E., and McKee, Adam. J.: A preliminary evaluation of
690 throughfall sampling techniques in a mature coniferous forest, *Journal of Forestry Research*, 25, 407–
691 413, <https://doi.org/10.1007/s11676-014-0468-8>, 2014.
- 692 Coenders-Gerrits, A. M. J., Hopp, L., Savenije, H. H. G., and Pfister, L.: The effect of spatial throughfall
693 patterns on soil moisture patterns at the hillslope scale, *Hydrol. Earth Syst. Sci.*, 17, 1749–1763,
694 <https://doi.org/10.5194/hess-17-1749-2013>, 2013.
- 695 Cosh, M. H., Jackson, T. J., Moran, S., and Bindlish, R.: Temporal persistence and stability of surface
696 soil moisture in a semi-arid watershed, *Remote Sensing of Environment*, 112, 304–313,
697 <https://doi.org/10.1016/j.rse.2007.07.001>, 2008.
- 698 Couvreur, V., Vanderborght, J., Beff, L., and Javaux, M.: Horizontal soil water potential heterogeneity:
699 simplifying approaches for crop water dynamics models, *Hydrology and Earth System Sciences*, 18,
700 1723–1743, <https://doi.org/10.5194/hess-18-1723-2014>, 2014.
- 701 Crockford, R. H. and Richardson, D. P.: Partitioning of rainfall into throughfall, stemflow and
702 interception: effect of forest type, ground cover and climate, *Hydrological Processes*, 14, 2903–2920,
703 2000.
- 704 Dawson, T. E.: Determining water use by trees and forests from isotopic, energy balance and transpiration
705 analyses: the roles of tree size and hydraulic lift, *Tree Physiology*, 16, 263–272,
706 <https://doi.org/10.1093/treephys/16.1-2.263>, 1996.
- 707 Demand, D., Blume, T., and Weiler, M.: Spatio-temporal relevance and controls of preferential flow at
708 the landscape scale, *Hydrol. Earth Syst. Sci.*, 23, 4869–4889, <https://doi.org/10.5194/hess-23-4869-2019>,
709 2019.
- 710 Demir, G., Michalzik, B., Filipzik, J., Metzger, J., and Hildebrandt, A.: Spatial variation of grassland
711 canopy affects soil wetting patterns and preferential flow,
712 <https://doi.org/10.22541/au.164970545.54927607/v1>, 2022.
- 713 Dunkerley, D.: Stemflow on the woody parts of plants: dependence on rainfall intensity and event profile
714 from laboratory simulations, *Hydrological Processes*, 28, 5469–5482, <https://doi.org/10.1002/hyp.10050>,
715 2014.
- 716 Emerman, S. H. and Dawson, T. E.: Hydraulic Lift and Its Influence on the Water Content of the
717 Rhizosphere: An Example from Sugar Maple, *Acer saccharum*, *Oecologia*, 108, 273–278, 1996.
- 718 Evaristo, J., Kim, M., van Haren, J., Pangle, L. A., Harman, C. J., Troch, P. A., and McDonnell, J. J.:
719 Characterizing the Fluxes and Age Distribution of Soil Water, Plant Water, and Deep Percolation in a
720 Model Tropical Ecosystem, *Water Resources Research*, 55, 3307–3327,
721 <https://doi.org/10.1029/2018WR023265>, 2019.

- 722 Fan, J., Oestergaard, K. T., Guyot, A., Jensen, D. G., and Lockington, D. A.: Spatial variability of
723 throughfall and stemflow in an exotic pine plantation of subtropical coastal Australia, *Hydrological*
724 *Processes*, 29, 793–804, <https://doi.org/10.1002/hyp.10193>, 2015.
- 725 .
- 726 Fischer-Bedtke, C., Metzger, J. C., Demir, G., Wutzler, T., and Hildebrandt, A.: Throughfall spatial
727 patterns translate into spatial patterns of soil moisture dynamics – empirical evidence, *Hydrology and*
728 *Earth System Sciences*, 27, 2899–2918, <https://doi.org/10.5194/hess-27-2899-2023>, 2023.
- 729 Forrester, D. I.: The spatial and temporal dynamics of species interactions in mixed-species forests: From
730 pattern to process, *Forest Ecology and Management*, 312, 282–292,
731 <https://doi.org/10.1016/j.foreco.2013.10.003>, 2014.
- 732 Forrester, D. I. and Bauhus, J.: A Review of Processes Behind Diversity—Productivity Relationships in
733 Forests, *Curr Forestry Rep*, 2, 45–61, <https://doi.org/10.1007/s40725-016-0031-2>, 2016.
- 734 Forrester, D. I., Theiveyanathan, S., Collopy, J. J., and Marcar, N. E.: Enhanced water use efficiency in a
735 mixed *Eucalyptus globulus* and *Acacia mearnsii* plantation, *Forest Ecology and Management*, 259, 1761–
736 1770, <https://doi.org/10.1016/j.foreco.2009.07.036>, 2010.
- 737 Gaines, K. P., Stanley, J. W., Meinzer, F. C., McCulloh, K. A., Woodruff, D. R., Chen, W., Adams, T.
738 S., Lin, H., and Eissenstat, D. M.: Reliance on shallow soil water in a mixed-hardwood forest in central
739 Pennsylvania, *Tree Physiol*, 36, 444–458, <https://doi.org/10.1093/treephys/tpv113>, 2016.
- 740 Gebauer, T., Horna, V., and Leuschner, C.: Canopy transpiration of pure and mixed forest stands with
741 variable abundance of European beech, *Journal of Hydrology*, 442–443, 2–14,
742 <https://doi.org/10.1016/j.jhydrol.2012.03.009>, 2012.
- 743 Gerrits, A. M. J., Pfister, L., and Savenije, H. H. G.: Spatial and temporal variability of canopy and forest
744 floor interception in a beech forest, *Hydrol. Process.*, 24, 3011–3025, <https://doi.org/10.1002/hyp.7712>,
745 2010.
- 746 González de Andrés, E., Camarero, J. J., Blanco, J. A., Imbert, J. B., Lo, Y.-H., Sangüesa-Barreda, G.,
747 and Castillo, F. J.: Tree-to-tree competition in mixed European beech–Scots pine forests has different
748 impacts on growth and water-use efficiency depending on site conditions, *Journal of Ecology*, 106, 59–
749 75, <https://doi.org/10.1111/1365-2745.12813>, 2018.
- 750 Grayson, R. B., Western, A. W., Chiew, F. H. S., and Blöschl, G.: Preferred states in spatial soil moisture
751 patterns: Local and nonlocal controls, *Water Resources Research*, 33, 2897–2908,
752 <https://doi.org/10.1029/97WR02174>, 1997.

- 753 Guderle, M. and Hildebrandt, A.: Using measured soil water contents to estimate evapotranspiration and
754 root water uptake profiles – a comparative study, *Hydrol. Earth Syst. Sci.*, 17, 2015.
- 755 Guderle, M., Bachmann, D., Milcu, A., Gockele, A., Bechmann, M., Fischer, C., Roscher, C., Landais,
756 D., Ravel, O., Devidal, S., Roy, J., Gessler, A., Buchmann, N., Weigelt, A., and Hildebrandt, A.: Dynamic
757 niche partitioning in root water uptake facilitates efficient water use in more diverse grassland plant
758 communities, *Funct Ecol*, 32, 214–227, <https://doi.org/10.1111/1365-2435.12948>, 2018.
- 759 Guo, J. S., Hungate, B. A., Kolb, T. E., and Koch, G. W.: Water source niche overlap increases with site
760 moisture availability in woody perennials, *Plant Ecol*, 219, 719–735, [https://doi.org/10.1007/s11258-018-](https://doi.org/10.1007/s11258-018-0829-z)
761 0829-z, 2018.
- 762 Guswa, A. J.: Canopy vs. Roots: Production and Destruction of Variability in Soil Moisture and
763 Hydrologic Fluxes, *Vadose Zone Journal*, 11, vzj2011.0159, <https://doi.org/10.2136/vzj2011.0159>, 2012.
- 764 Guswa, A. J. and Spence, C. M.: Effect of throughfall variability on recharge: application to hemlock and
765 deciduous forests in western Massachusetts, *Ecohydrology*, 5, 563–574, <https://doi.org/10.1002/eco.281>,
766 2012.
- 767 Hafner, B. D., Tomasella, M., Häberle, K.-H., Goebel, M., Matyssek, R., and Grams, T. E. E.: Hydraulic
768 redistribution under moderate drought among English oak, European beech and Norway spruce
769 determined by deuterium isotope labeling in a split-root experiment, *Tree Physiology*, 37, 950–960,
770 <https://doi.org/10.1093/treephys/tpx050>, 2017.
- 771 Hafner, B. D., Hesse, B. D., and Grams, T. E. E.: Friendly neighbours: Hydraulic redistribution accounts
772 for one quarter of water used by neighbouring drought stressed tree saplings, *Plant, Cell & Environment*,
773 44, 1243–1256, <https://doi.org/10.1111/pce.13852>, 2021.
- 774 Hildebrandt, A.: Root-Water Relations and Interactions in Mixed Forest Settings, in: *Forest-Water*
775 *Interactions*, edited by: Levia, D. F., Carlyle-Moses, D. E., Iida, S., Michalzik, B., Nanko, K., and Tischer,
776 A., Springer International Publishing, Cham, 319–348, https://doi.org/10.1007/978-3-030-26086-6_14,
777 2020.
- 778 Hildebrandt, A., Kleidon, A., and Bechmann, M.: A thermodynamic formulation of root water uptake,
779 *Hydrol. Earth Syst. Sci.*, 14, 2016.
- 780 Hopmans, J. W. and Bristow, K. L.: Current Capabilities and Future Needs of Root Water and Nutrient
781 Uptake Modeling, in: *Advances in Agronomy*, vol. 77, Elsevier, 103–183, [https://doi.org/10.1016/S0065-](https://doi.org/10.1016/S0065-2113(02)77014-4)
782 2113(02)77014-4, 2002.
- 783 Hupet, F. and Vanclooster, M.: Micro-variability of hydrological processes at the maize row scale:
784 implications for soil water content measurements and evapotranspiration estimates, *Journal of Hydrology*,
785 303, 247–270, <https://doi.org/10.1016/j.jhydrol.2004.07.017>, 2005.

- 786 Hupet, F., Lambot, S., Javaux, M., and Vanclooster, M.: On the identification of macroscopic root water
787 uptake parameters from soil water content observations, *Water Resources Research*, 38, 36-1-36-14,
788 <https://doi.org/10.1029/2002WR001556>, 2002.
- 789 IUSS Working Group, W. and others: World reference base for soil resources, *World Soil Resources*
790 *Report*, 103, 2006.
- 791 Ivanov, V. Y., Fatichi, S., Jenerette, G. D., Espeleta, J. F., Troch, P. A., and Huxman, T. E.: Hysteresis
792 of soil moisture spatial heterogeneity and the “homogenizing” effect of vegetation, *Water Resources*
793 *Research*, 46, <https://doi.org/10.1029/2009WR008611>, 2010.
- 794 Jackisch, C., Knoblauch, S., Blume, T., Zehe, E., and Hassler, S. K.: Estimates of tree root water uptake
795 from soil moisture profile dynamics, *Biogeosciences*, 17, 5787–5808, <https://doi.org/10.5194/bg-17-5787-2020>, 2020.
- 797 Jarecke, K. M., Bladon, K. D., and Wondzell, S. M.: The Influence of Local and Nonlocal Factors on Soil
798 Water Content in a Steep Forested Catchment, *Water Resources Research*, 57, e2020WR028343,
799 <https://doi.org/10.1029/2020WR028343>, 2021.
- 800 Jonard, F., André, F., Ponette, Q., Vincke, C., and Jonard, M.: Sap flux density and stomatal conductance
801 of European beech and common oak trees in pure and mixed stands during the summer drought of 2003,
802 *Journal of Hydrology*, 409, 371–381, <https://doi.org/10.1016/j.jhydrol.2011.08.032>, 2011.
- 803 Jost, G., Schume, H., and Hager, H.: Factors controlling soil water-recharge in a mixed European beech
804 (*Fagus sylvatica* L.)–Norway spruce [*Picea abies* (L.) Karst.] stand, *Eur J Forest Res*, 123, 93–104,
805 <https://doi.org/10.1007/s10342-004-0033-7>, 2004.
- 806 Katul, G. G. and Siqueira, M. B.: Biotic and abiotic factors act in coordination to amplify hydraulic
807 redistribution and lift, *The New Phytologist*, 187, 3–6, 2010.
- 808 Keim, R. F., Skaugset, A. E., and Weiler, M.: Temporal persistence of spatial patterns in throughfall,
809 *Journal of Hydrology*, 314, 263–274, <https://doi.org/10.1016/j.jhydrol.2005.03.021>, 2005.
- 810 Keim, R. F., Skaugset, A. E., and Weiler, M.: Storage of water on vegetation under simulated rainfall of
811 varying intensity, *Advances in Water Resources*, 29, 974–986,
812 <https://doi.org/10.1016/j.advwatres.2005.07.017>, 2006.
- 813 Kirchen, G., Calvaruso, C., Granier, A., Redon, P.-O., Van der Heijden, G., Bréda, N., and Turpault, M.-
814 P.: Local soil type variability controls the water budget and stand productivity in a beech forest, *Forest*
815 *Ecology and Management*, 390, 89–103, <https://doi.org/10.1016/j.foreco.2016.12.024>, 2017.

- 816 Kleidon, A. and Renner, M.: Thermodynamic limits of hydrologic cycling within the Earth system:
817 concepts, estimates and implications, *Hydrol. Earth Syst. Sci.*, 17, 2873–2892,
818 <https://doi.org/10.5194/hess-17-2873-2013>, 2013.
- 819 Kleidon, A., Renner, M., and Porada, P.: Estimates of the climatological land surface energy and water
820 balance derived from maximum convective power, *Hydrol. Earth Syst. Sci.*, 18, 2201–2218,
821 <https://doi.org/10.5194/hess-18-2201-2014>, 2014.
- 822 Klein, T., Rotenberg, E., Cohen-Hilaleh, E., Raz-Yaseef, N., Tatarinov, F., Preisler, Y., Ogée, J., Cohen,
823 S., and Yakir, D.: Quantifying transpirable soil water and its relations to tree water use dynamics in a
824 water-limited pine forest, *Ecohydrology*, 7, 409–419, <https://doi.org/10.1002/eco.1360>, 2014.
- 825 Knighton, J., Singh, K., and Evaristo, J.: Understanding Catchment-Scale Forest Root Water Uptake
826 Strategies Across the Continental United States Through Inverse Ecohydrological Modeling, *Geophysical*
827 *Research Letters*, 47, e2019GL085937, <https://doi.org/10.1029/2019GL085937>, 2019.
- 828 Kohlhepp, B., Lehmann, R., Seeber, P., Küsel, K., Trumbore, S. E., and Totsche, K. U.: Aquifer
829 configuration and geostructural links control the groundwater quality in thin-bedded carbonate–
830 siliciclastic alternations of the Hainich CZE, central Germany, *Hydrol. Earth Syst. Sci.*, 21, 6091–6116,
831 <https://doi.org/10.5194/hess-21-6091-2017>, 2017.
- 832 Kostner, B., Falge, E., and Tenhunen, J. D.: Age-related effects on leaf area/sapwood area relationships,
833 canopy transpiration and carbon gain of Norway spruce stands (*Picea abies*) in the Fichtelgebirge,
834 Germany, *Tree Physiology*, 22, 567–574, <https://doi.org/10.1093/treephys/22.8.567>, 2002.
- 835 Krämer, I. and Hölscher, D.: Soil water dynamics along a tree diversity gradient in a deciduous forest in
836 Central Germany, *Ecohydrology*, 3, 262–271, <https://doi.org/10.1002/eco.103>, 2010.
- 837 Kreuzwieser, J. and Gessler, A.: Global climate change and tree nutrition: influence of water availability,
838 *Tree Physiology*, 30, 1221–1234, <https://doi.org/10.1093/treephys/tpq055>, 2010.
- 839 Kühnhammer, K., Kübert, A., Brüggemann, N., Deseano Diaz, P., van Dusschoten, D., Javaux, M., Merz,
840 S., Vereecken, H., Dubbert, M., and Rothfuss, Y.: Investigating the root plasticity response of *Centaurea*
841 *jacea* to soil water availability changes from isotopic analysis, *New Phytologist*, 226, 98–110,
842 <https://doi.org/10.1111/nph.16352>, 2020.
- 843 Kunert, N., Schwendenmann, L., Potvin, C., and Hölscher, D.: Tree diversity enhances tree transpiration
844 in a Panamanian forest plantation, *Journal of Applied Ecology*, 49, 135–144,
845 <https://doi.org/10.1111/j.1365-2664.2011.02065.x>, 2012.
- 846 Küsel, K., Totsche, K. U., Trumbore, S. E., Lehmann, R., Steinhäuser, C., and Herrmann, M.: How Deep
847 Can Surface Signals Be Traced in the Critical Zone? Merging Biodiversity with Biogeochemistry

- 848 Research in a Central German Muschelkalk Landscape, *Frontiers in Earth Science*, 4,
849 <https://doi.org/10.3389/feart.2016.00032>, 2016.
- 850 Le Goff, N. and Ottorini, J.-M.: Root biomass and biomass increment in a beech (*Fagus sylvatica* L.)
851 stand in North-East France, *Ann. For. Sci.*, 58, 1–13, <https://doi.org/10.1051/forest:2001104>, 2001.
- 852 Lee, E., Kumar, P., Barron-Gafford, G. A., Hendryx, S. M., Sanchez-Cañete, E. P., Minor, R. L., Colella,
853 T., and Scott, R. L.: Impact of Hydraulic Redistribution on Multispecies Vegetation Water Use in a
854 Semiarid Savanna Ecosystem: An Experimental and Modeling Synthesis, *Water Resour. Res.*, 54, 4009–
855 4027, <https://doi.org/10.1029/2017WR021006>, 2018.
- 856 Leuschner, C.: Drought response of European beech (*Fagus sylvatica* L.)—A review, *Perspectives in*
857 *Plant Ecology, Evolution and Systematics*, 47, 125576, <https://doi.org/10.1016/j.ppees.2020.125576>,
858 2020.
- 859 Levia, D. F. and Frost, E. E.: A review and evaluation of stemflow literature in the hydrologic and
860 biogeochemical cycles of forested and agricultural ecosystems, *Journal of Hydrology*, 274, 1–29,
861 [https://doi.org/10.1016/S0022-1694\(02\)00399-2](https://doi.org/10.1016/S0022-1694(02)00399-2), 2003.
- 862 Levia, D. F. and Frost, E. E.: Variability of throughfall volume and solute inputs in wooded ecosystems,
863 *Progress in Physical Geography: Earth and Environment*, 30, 605–632,
864 <https://doi.org/10.1177/0309133306071145>, 2006.
- 865 Levia, D. F., Keim, R. F., Carlyle-Moses, D. E., and Frost, E. E.: Throughfall and Stemflow in Wooded
866 Ecosystems, in: *Forest Hydrology and Biogeochemistry: Synthesis of Past Research and Future*
867 *Directions*, edited by: Levia, D. F., Carlyle-Moses, D., and Tanaka, T., Springer Netherlands, Dordrecht,
868 425–443, https://doi.org/10.1007/978-94-007-1363-5_21, 2011.
- 869 Levia, D. F., Hudson, S. A., Llorens, P., and Nanko, K.: Throughfall drop size distributions: a review and
870 prospectus for future research: Throughfall drop size distributions, *WIREs Water*, 4, e1225,
871 <https://doi.org/10.1002/wat2.1225>, 2017.
- 872 Lhomme, J.-P.: Formulation of root water uptake in a multi-layer soil-plant model: does van den Honert's
873 equation hold?, *Hydrology and Earth System Sciences*, 2, 31–39, <https://doi.org/10.5194/hess-2-31-1998>,
874 1998.
- 875 Looy, K. V., Bouma, J., Herbst, M., Koestel, J., Minasny, B., Mishra, U., Montzka, C., Nemes, A.,
876 Pachepsky, Y. A., Padarian, J., Schaap, M. G., Tóth, B., Verhoef, A., Vanderborght, J., Ploeg, M. J. van
877 der, Weihermüller, L., Zacharias, S., Zhang, Y., and Vereecken, H.: Pedotransfer Functions in Earth
878 System Science: Challenges and Perspectives, *Reviews of Geophysics*, 55, 1199–1256,
879 <https://doi.org/10.1002/2017RG000581>, 2017.

- 880 Lübke, T., Schuldt, B., Coners, H., and Leuschner, C.: Species diversity and identity effects on the water
881 consumption of tree sapling assemblages under ample and limited water supply, *Oikos*, 125, 86–97,
882 <https://doi.org/10.1111/oik.02367>, 2016.
- 883 Lüdecke, D., Ben-Shachar, M., Patil, I., Waggoner, P., and Makowski, D.: performance: An R Package
884 for Assessment, Comparison and Testing of Statistical Models, *JOSS*, 6, 3139,
885 <https://doi.org/10.21105/joss.03139>, 2021.
- 886 Magh, R.-K., Eiferle, C., Burzlaff, T., Dannenmann, M., Rennenberg, H., and Dubbert, M.: Competition
887 for water rather than facilitation in mixed beech-fir forests after drying-wetting cycle, *Journal of*
888 *Hydrology*, 587, 124944, <https://doi.org/10.1016/j.jhydrol.2020.124944>, 2020.
- 889 Magliano, P. N., Whitworth-Hulse, J. I., Florio, E. L., Aguirre, E. C., and Blanco, L. J.: Interception loss,
890 throughfall and stemflow by *Larrea divaricata*: The role of rainfall characteristics and plant morphological
891 attributes, *Ecological Research*, 34, 753–764, <https://doi.org/10.1111/1440-1703.12036>, 2019.
- 892 Martínez García, G., Pachepsky, Y. A., and Vereecken, H.: Effect of soil hydraulic properties on the
893 relationship between the spatial mean and variability of soil moisture, *Journal of Hydrology*, 516, 154–
894 160, <https://doi.org/10.1016/j.jhydrol.2014.01.069>, 2014.
- 895 Meinen, C., Leuschner, C., Ryan, N. T., and Hertel, D.: No evidence of spatial root system segregation
896 and elevated fine root biomass in multi-species temperate broad-leaved forests, *Trees*, 23, 941–950,
897 <https://doi.org/10.1007/s00468-009-0336-x>, 2009.
- 898 Meißner, M., Köhler, M., Schwendenmann, L., and Hölscher, D.: Partitioning of soil water among canopy
899 trees during a soil desiccation period in a temperate mixed forest, *Biogeosciences*, 9, 3465–3474,
900 <https://doi.org/10.5194/bg-9-3465-2012>, 2012.
- 901 Metzger, J. C., Wutzler, T., Valle, N. D., Filipzik, J., Grauer, C., Lehmann, R., Roggenbuck, M.,
902 Schelhorn, D., Weckmüller, J., Küsel, K., Totsche, K. U., Trumbore, S., and Hildebrandt, A.: Vegetation
903 impacts soil water content patterns by shaping canopy water fluxes and soil properties, *Hydrological*
904 *Processes*, 31, 3783–3795, <https://doi.org/10.1002/hyp.11274>, 2017.
- 905 Metzger, J. C., Filipzik, J., Michalzik, B., and Hildebrandt, A.: Stemflow Infiltration Hotspots Create Soil
906 Microsites Near Tree Stems in an Unmanaged Mixed Beech Forest, *Front. For. Glob. Change*, 4, 701293,
907 <https://doi.org/10.3389/ffgc.2021.701293>, 2021.
- 908 Molina, A. J., Llorens, P., Garcia-Estringana, P., Moreno de las Heras, M., Cayuela, C., Gallart, F., and
909 Latron, J.: Contributions of throughfall, forest and soil characteristics to near-surface soil water-content
910 variability at the plot scale in a mountainous Mediterranean area, *Science of The Total Environment*, 647,
911 1421–1432, <https://doi.org/10.1016/j.scitotenv.2018.08.020>, 2019.

- 912 Nadezhdina, N., Cermak, J., Meiresonne, L., and Ceulemans, R.: Transpiration of Scots pine in Flanders
913 growing on soil with irregular substratum, *Forest Ecology and Management*, 9, 2007.
- 914 Neumann, R. B. and Cardon, Z. G.: The magnitude of hydraulic redistribution by plant roots: a review
915 and synthesis of empirical and modeling studies, *New Phytologist*, 194, 337–352,
916 <https://doi.org/10.1111/j.1469-8137.2012.04088.x>, 2012.
- 917 Nie, C., Huang, Y., Zhang, S., Yang, Y., Zhou, S., Lin, C., and Wang, G.: Effects of soil water content
918 on forest ecosystem water use efficiency through changes in transpiration/evapotranspiration ratio,
919 *Agricultural and Forest Meteorology*, 308–309, 108605,
920 <https://doi.org/10.1016/j.agrformet.2021.108605>, 2021.
- 921 Obladen, N., Dechering, P., Skiadaresis, G., Tegel, W., Keßler, J., Höllerl, S., Kaps, S., Hertel, M.,
922 Dulamsuren, C., Seifert, T., Hirsch, M., and Seim, A.: Tree mortality of European beech and Norway
923 spruce induced by 2018–2019 hot droughts in central Germany, *Agricultural and Forest Meteorology*,
924 307, 108482, <https://doi.org/10.1016/j.agrformet.2021.108482>, 2021.
- 925 Otto, J., Berveiller, D., Bréon, F.-M., Delpierre, N., Geppert, G., Granier, A., Jans, W., Knohl, A., Kuusk,
926 A., Longdoz, B., Moors, E., Mund, M., Pinty, B., Schelhaas, M.-J., and Luysaert, S.: Forest summer
927 albedo is sensitive to species and thinning: how should we account for this in Earth system models?,
928 *Biogeosciences*, 11, 2411–2427, <https://doi.org/10.5194/bg-11-2411-2014>, 2014.
- 929 Pearson, R. K.: Data cleaning for dynamic modeling and control, in: 1999 European Control Conference
930 (ECC), 1999 European Control Conference (ECC), 2584–2589,
931 <https://doi.org/10.23919/ECC.1999.7099714>, 1999.
- 932 Pretzsch, H., Schütze, G., and Uhl, E.: Resistance of European tree species to drought stress in mixed
933 versus pure forests: evidence of stress release by inter-specific facilitation, *Plant Biology*, 15, 483–495,
934 <https://doi.org/10.1111/j.1438-8677.2012.00670.x>, 2013.
- 935 Priyadarshini, K. V. R., Prins, H. H. T., de Bie, S., Heitkönig, I. M. A., Woodborne, S., Gort, G., Kirkman,
936 K., Ludwig, F., Dawson, T. E., and de Kroon, H.: Seasonality of hydraulic redistribution by trees to
937 grasses and changes in their water-source use that change tree-grass interactions: HYDRAULIC
938 REDISTRIBUTION BY TREES TO GRASSES AND CHANGES IN THEIR WATER SOURCES,
939 *Ecohydrology*, 9, 218–228, <https://doi.org/10.1002/eco.1624>, 2016.
- 940 Pypker, T. G., Levia, D. F., Staelens, J., and Van Stan, J. T.: Canopy Structure in Relation to Hydrological
941 and Biogeochemical Fluxes, in: *Forest Hydrology and Biogeochemistry: Synthesis of Past Research and
942 Future Directions*, edited by: Levia, D. F., Carlyle-Moses, D., and Tanaka, T., Springer Netherlands,
943 Dordrecht, 371–388, https://doi.org/10.1007/978-94-007-1363-5_18, 2011.
- 944 R Core Team: R: The R Project for Statistical Computing, R Foundation for Statistical Computing,
945 Vienna, Austria, 2021.

- 946 Raat, K. J., Draaijers, G. P. J., Schaap, M. G., Tietema, A., and Verstraten, J. M.: Spatial variability of
947 throughfall water and chemistry and forest floor water content in a Douglas fir forest stand, *Hydrol. Earth*
948 *Syst. Sci.*, 6, 363–374, <https://doi.org/10.5194/hess-6-363-2002>, 2002.
- 949 del Río, M., Schütze, G., and Pretzsch, H.: Temporal variation of competition and facilitation in mixed
950 species forests in Central Europe, *Plant Biology*, 16, 166–176, <https://doi.org/10.1111/plb.12029>, 2014.
- 951 Rodrigues, A. F., Terra, M. C. N. S., Mantovani, V. A., Cordeiro, N. G., Ribeiro, J. P. C., Guo, L., Nehren,
952 U., Mello, J. M., and Mello, C. R.: Throughfall spatial variability in a neotropical forest: Have we
953 correctly accounted for time stability?, *Journal of Hydrology*, 608, 127632,
954 <https://doi.org/10.1016/j.jhydrol.2022.127632>, 2022.
- 955 Rodríguez-Robles, U., Arredondo, J. T., Huber-Sannwald, E., Yépez, E. A., and Ramos-Leal, J. A.:
956 Coupled plant traits adapted to wetting/drying cycles of substrates co-define niche multidimensionality,
957 *Plant, Cell & Environment*, 43, 2394–2408, <https://doi.org/10.1111/pce.13837>, 2020.
- 958 Rosenbaum, U., Bogena, H. R., Herbst, M., Huisman, J. A., Peterson, T. J., Weuthen, A., Western, A.
959 W., and Vereecken, H.: Seasonal and event dynamics of spatial soil moisture patterns at the small
960 catchment scale: DYNAMICS OF CATCHMENT-SCALE SOIL MOISTURE PATTERNS, *Water*
961 *Resour. Res.*, 48, <https://doi.org/10.1029/2011WR011518>, 2012.
- 962 Rothfuss, Y. and Javaux, M.: Reviews and syntheses: Isotopic approaches to quantify root water uptake:
963 a review and comparison of methods, *Biogeosciences*, 14, 2199–2224, [https://doi.org/10.5194/bg-14-](https://doi.org/10.5194/bg-14-2199-2017)
964 [2199-2017](https://doi.org/10.5194/bg-14-2199-2017), 2017.
- 965 Sadeghi, S. M. M., Gordon, D. A., and Van Stan II, J. T.: A Global Synthesis of Throughfall and Stemflow
966 Hydrometeorology, in: *Precipitation Partitioning by Vegetation: A Global Synthesis*, edited by: Van Stan,
967 I., John T., Gutmann, E., and Friesen, J., Springer International Publishing, Cham, 49–70,
968 https://doi.org/10.1007/978-3-030-29702-2_4, 2020.
- 969 Schume, H., Jost, G., and Hager, H.: Soil water depletion and recharge patterns in mixed and pure forest
970 stands of European beech and Norway spruce, *Journal of Hydrology*, 289, 258–274,
971 <https://doi.org/10.1016/j.jhydrol.2003.11.036>, 2004.
- 972 Schwärzel, K., Menzer, A., Clausnitzer, F., Spank, U., Häntzschel, J., Grünwald, T., Köstner, B.,
973 Bernhofer, C., and Feger, K.-H.: Soil water content measurements deliver reliable estimates of water
974 fluxes: A comparative study in a beech and a spruce stand in the Tharandt forest (Saxony, Germany),
975 *Agricultural and Forest Meteorology*, 149, 1994–2006, <https://doi.org/10.1016/j.agrformet.2009.07.006>,
976 2009.
- 977 Seeger, S. and Weiler, M.: Temporal dynamics of tree xylem water isotopes: in situ monitoring and
978 modeling, *Biogeosciences*, 18, 4603–4627, <https://doi.org/10.5194/bg-18-4603-2021>, 2021.

- 979 Shachnovich, Y., Berliner, P. R., and Bar, P.: Rainfall interception and spatial distribution of throughfall
980 in a pine forest planted in an arid zone, *Journal of Hydrology*, 349, 168–177,
981 <https://doi.org/10.1016/j.jhydrol.2007.10.051>, 2008.
- 982 Shani, U. and Dudley, L. M.: Modeling water uptake by roots under water and salt stress: Soil-based and
983 crop response root sink terms, *Plant Roots: The Hidden Half*, 635–641, 1996.
- 984 Silvertown, J., Araya, Y., and Gowing, D.: Hydrological niches in terrestrial plant communities: a review,
985 *Journal of Ecology*, 103, 93–108, <https://doi.org/10.1111/1365-2745.12332>, 2015.
- 986 Spanner, G. C., Gimenez, B. O., Wright, C. L., Menezes, V. S., Newman, B. D., Collins, A. D., Jardine,
987 K. J., Negrón-Juárez, R. I., Lima, A. J. N., Rodrigues, J. R., Chambers, J. Q., Higuchi, N., and Warren, J.
988 M.: Dry Season Transpiration and Soil Water Dynamics in the Central Amazon, *Frontiers in Plant
989 Science*, 13, 2022.
- 990 Sprenger, M., Llorens, P., Cayuela, C., Gallart, F., and Latron, J.: Mechanisms of consistently disjunct
991 soil water pools over (pore) space and time, *Hydrol. Earth Syst. Sci.*, 23, 2751–2762,
992 <https://doi.org/10.5194/hess-23-2751-2019>, 2019.
- 993 Staelens, J., De Schrijver, A., Verheyen, K., and Verhoest, N. E. C.: Spatial variability and temporal
994 stability of throughfall water under a dominant beech (*Fagus sylvatica* L.) tree in relationship to canopy
995 cover, *Journal of Hydrology*, 330, 651–662, <https://doi.org/10.1016/j.jhydrol.2006.04.032>, 2006.
- 996 Staelens, J., De Schrijver, A., Verheyen, K., and Verhoest, N. E. C.: Rainfall partitioning into throughfall,
997 stemflow, and interception within a single beech (*Fagus sylvatica* L.) canopy: influence of foliation, rain
998 event characteristics, and meteorology, *Hydrological Processes*, 22, 33–45,
999 <https://doi.org/10.1002/hyp.6610>, 2008.
- 1000 Teuling, A. J. and Troch, P. A.: Improved understanding of soil moisture variability dynamics,
1001 *Geophysical Research Letters*, 32, <https://doi.org/10.1029/2004GL021935>, 2005.
- 1002 Thiurmel, B. and Elmarhraoui, A.: *suncalc: Compute Sun Position, Sunlight Phases, Moon Position and
1003 Lunar Phase*, 2022.
- 1004 Tsuruta, K., Kwon, H., Law, B. E., and Kume, T.: Relationship between stem diameter and whole-tree
1005 transpiration across young, mature and old-growth ponderosa pine forests under wet and dry soil
1006 conditions, *Ecohydrology*, e2572, <https://doi.org/10.1002/eco.2572>, 2023.
- 1007 Vachaud, G., Passerat De Silans, A., Balabanis, P., and Vauclin, M.: Temporal Stability of Spatially
1008 Measured Soil Water Probability Density Function, *Soil Science Society of America Journal*, 49, 822–
1009 828, <https://doi.org/10.2136/sssaj1985.03615995004900040006x>, 1985.

- 1010 Van Stan, J. T., Siegert, C. M., Levia, D. F., and Scheick, C. E.: Effects of wind-driven rainfall on
1011 stemflow generation between codominant tree species with differing crown characteristics, *Agricultural*
1012 *and Forest Meteorology*, 151, 1277–1286, <https://doi.org/10.1016/j.agrformet.2011.05.008>, 2011.
- 1013 Van Stan, J. T., Hildebrandt, A., Friesen, J., Metzger, J. C., and Yankine, S. A.: Spatial Variability and
1014 Temporal Stability of Local Net Precipitation Patterns, in: *Precipitation Partitioning by Vegetation: A*
1015 *Global Synthesis*, edited by: Van Stan, I., John T., Gutmann, E., and Friesen, J., Springer International
1016 Publishing, Cham, 89–104, https://doi.org/10.1007/978-3-030-29702-2_6, 2020.
- 1017 Vereecken, H., Kamai, T., Harter, T., Kasteel, R., Hopmans, J., and Vanderborght, J.: Explaining soil
1018 moisture variability as a function of mean soil moisture: A stochastic unsaturated flow perspective,
1019 *Geophysical Research Letters*, 34, <https://doi.org/10.1029/2007GL031813>, 2007.
- 1020 Vereecken, H., Amelung, W., Bauke, S. L., Bogena, H., Brüggemann, N., Montzka, C., Vanderborght,
1021 J., Bechtold, M., Blöschl, G., Carminati, A., Javaux, M., Konings, A. G., Kusche, J., Neuweiler, I., Or,
1022 D., Steele-Dunne, S., Verhoef, A., Young, M., and Zhang, Y.: Soil hydrology in the Earth system, *Nat*
1023 *Rev Earth Environ*, 3, 573–587, <https://doi.org/10.1038/s43017-022-00324-6>, 2022.
- 1024 Vitali, V., Forrester, D. I., and Bauhus, J.: Know Your Neighbours: Drought Response of Norway Spruce,
1025 Silver Fir and Douglas Fir in Mixed Forests Depends on Species Identity and Diversity of Tree
1026 Neighbourhoods, *Ecosystems*, 21, 1215–1229, <https://doi.org/10.1007/s10021-017-0214-0>, 2018.
- 1027 Volkman, T. H. M., Haberer, K., Gessler, A., and Weiler, M.: High-resolution isotope measurements
1028 resolve rapid ecohydrological dynamics at the soil–plant interface, *New Phytologist*, 210, 839–849,
1029 <https://doi.org/10.1111/nph.13868>, 2016.
- 1030 Wambsganss, J., Beyer, F., Freschet, G. T., Scherer-Lorenzen, M., and Bauhus, J.: Tree species mixing
1031 reduces biomass but increases length of absorptive fine roots in European forests, *J Ecol*, 109, 2678–
1032 2691, <https://doi.org/10.1111/1365-2745.13675>, 2021.
- 1033 Whelan, M. J. and Anderson, J. M.: Modelling spatial patterns of throughfaU and interception loss in a
1034 Norway spruce (*Picea abies*) plantation at the plot scale, *Journal of Hydrology*, 186, 335–354, 1996.
- 1035 Wiekenkamp, I., Huisman, J. A., Bogena, H. R., Lin, H. S., and Vereecken, H.: Spatial and temporal
1036 occurrence of preferential flow in a forested headwater catchment, *Journal of Hydrology*, 534, 139–149,
1037 <https://doi.org/10.1016/j.jhydrol.2015.12.050>, 2016.
- 1038 Wullaert, H., Pohlert, T., Boy, J., Valarezo, C., and Wilcke, W.: Spatial throughfall heterogeneity in a
1039 montane rain forest in Ecuador: Extent, temporal stability and drivers, *Journal of Hydrology*, 377, 71–79,
1040 <https://doi.org/10.1016/j.jhydrol.2009.08.001>, 2009.
- 1041 Yu, K. and D’Odorico, P.: Hydraulic lift as a determinant of tree–grass coexistence on savannas, *New*
1042 *Phytologist*, 207, 1038–1051, <https://doi.org/10.1111/nph.13431>, 2015.

- 1043 Zacharias, S. and Wessolek, G.: Excluding Organic Matter Content from Pedotransfer Predictors of Soil
1044 Water Retention, *Soil Science Society of America Journal*, 71, 43–50,
1045 <https://doi.org/10.2136/sssaj2006.0098>, 2007.
- 1046 Zarebanadkouki, M., Kim, Y. X., and Carminati, A.: Where do roots take up water? Neutron radiography
1047 of water flow into the roots of transpiring plants growing in soil, *New Phytologist*, 199, 1034–1044,
1048 <https://doi.org/10.1111/nph.12330>, 2013.
- 1049 Zehe, E., Graeff, T., Morgner, M., Bauer, A., and Bronstert, A.: Plot and field scale soil moisture
1050 dynamics and subsurface wetness control on runoff generation in a headwater in the Ore Mountains,
1051 *Hydrol. Earth Syst. Sci.*, 14, 873–889, <https://doi.org/10.5194/hess-14-873-2010>, 2010.
- 1052 Zhang, Y., Wang, X., Hu, R., and Pan, Y.: Throughfall and its spatial variability beneath xerophytic shrub
1053 canopies within water-limited arid desert ecosystems, *Journal of Hydrology*, 539, 406–416,
1054 <https://doi.org/10.1016/j.jhydrol.2016.05.051>, 2016.
- 1055 Zhu, X., He, Z., Du, J., Chen, L., Lin, P., and Tian, Q.: Spatial heterogeneity of throughfall and its
1056 contributions to the variability in near-surface soil water-content in semiarid mountains of China, *Forest
1057 Ecology and Management*, 488, 119008, <https://doi.org/10.1016/j.foreco.2021.119008>, 2021.
- 1058 Zimmermann, A., Zimmermann, B., and Elsenbeer, H.: Rainfall redistribution in a tropical forest: Spatial
1059 and temporal patterns, *Water Resour. Res.*, 45, <https://doi.org/10.1029/2008WR007470>, 2009.
- 1060 Zuur, A. F., Ieno, E. N., Walker, N., Saveliev, A. A., and Smith, G. M.: Mixed effects models and
1061 extensions in ecology with R, Springer New York, New York, NY, <https://doi.org/10.1007/978-0-387-87458-6>, 2009.

1063